Beneficial effect of indigo naturalis on acute lung injury induced by influenza A virus

Peng Tu
Fudan University School of Pharmacy
Rong Tian
Fudan University School of Pharmacy
Yan Lu
Fudan University School of Pharmacy
Yunyi Zhang
Fudan University School of Pharmacy
Haiyan Zhu
Fudan University School of Pharmacy
Lijun Ling
Fudan University School of Pharmacy
Hong Li
Fudan University School of Pharmacy
Daofeng Chen (dfchen@shmu.edu.cn)
Fudan University School of Pharmacy

Research

Keywords: influenza, indigo naturalis, acute lune injury, cytokines, COVID-19

Posted Date: November 6th, 2020

DOI: https://doi.org/10.21203/rs.3.rs-73166/v2

Version of Record: A version of this preprint was published on December 21st, 2020. See the published version at https://doi.org/10.1186/s13020-020-00415-w.

Abstract

Background: Infections induced by influenza viruses, as well as coronavirus disease 19 (COVID-19) pandemic induced by severe acute respiratory coronavirus 2 (SARS-CoV-2) led to acute lung injury (ALI) and multi organ failure, during which traditional Chinese medicine (TCM) played an important role in treatment of the pandemic. The study aimed to investigate the effect of indigo naturalis on ALI induced by influenza A virus (IAV) in mice.

Method: The anti-influenza and anti-inflammatory properties of aqueous extract of indigo naturalis (INAE) were evaluated *in vitro*. BALB/c mice inoculated intranasally with IAV (H1N1) were treated intragastrically with INAE (40, 80 and 160 mg·kg^{-1}/d) 2 h later for 4 or 7 days. Animal lifespan and mortality were recorded. Expression of high mobility group box-1 protein (HMGB-1) and toll-like receptor 4 (TLR4) were evaluated through immunohistological staining. Inflammatory cytokines were also monitored by ELISA.

Result: INAE inhibited virus replication on Madin-Darby canine kidney (MDCK) cells and decreased nitric oxide (NO) production from lipopolysaccharide (LPS)-stimulated peritoneal macrophages *in vitro*. The results showed that oral administration of 160 mg/kg of INAE significantly improved the lifespan ($P < 0.01$) and survival rate of IAV infected mice, improved lung injury and lowered viral replication in lung tissue ($P < 0.01$). Treatment with INAE (40, 80 and 160 mg/kg) significantly increased liver weight and liver index ($P < 0.05$), as well as weight and organ index of thymus and spleen at 160 mg/kg ($P < 0.05$). Serum alanine transaminase (ALT) and aspartate aminotransferase (AST) levels were reduced by INAE administration ($P < 0.05$). The expression of HMGB-1 and TLR4 in lung tissue were also suppressed. The increased production of myeloperoxidase (MPO) and methylene dioxyamphetamine (MDA) in lung tissue were inhibited by INAE treatment ($P < 0.05$). Treatment with INAE reduced the high levels of interferon α (IFN-α), interferon β (IFN-β), monocyte chemoattractant protein-1 (MCP-1), regulated upon activation normal T cell expressed and secreted factor (RANTES), interferon induced protein-10 (IP-10), tumor necrosis factor-α (TNF-α), interleukin-6 (IL-6) ($P < 0.05$), with increased production of interferon γ (IFN-γ) and interleukin-10 (IL-10) ($P < 0.05$).

Conclusion: The results showed that INae alleviated IAV induced ALI in mice. The effect of INAE might be related with its anti-influenza, anti-inflammatory and anti-oxidation properties, which give a hint that indigo naturalis might be effective on respiratory viruses infected acute lung injury or SAR-CoV-2 caused COVID-19.

Background

Viruses infection has threatened human health. The current outbreak of novel coronavirus disease 19 (COVID-19), caused by severe acute respiratory coronavirus 2 (SARS-CoV-2), has become a big threat to the world [1]. The growing infection is second only to the influenza virus infection occurred in 1918, which killed more than 50 billion people worldwide, and resulted in havoc with military operations during the First World War [2]

Influenza A virus (IAV) is one of the important human pathogens worldwide. IAV infection can cause acute respiratory distress syndrome (ARDS), pneumonia, and lead to high mortality and morbidity [3]. Just like the current coronavirus pandemic which has spread over 200 countries and regions, fast spread of IAV infection may cause epidemic and threat people's safety and property [4].

IAV is negative strand RNA virus belonging to the family of orthomyxoviridae with a genome consisting of eight single stranded RNA segments of negative polarity [5]. Vaccine, M2 ion channel inhibitors and neuraminidase inhibitors are most used for treatment of IAV infection [6]. However, the lack of timeliness of vaccines and continuous records about drug resistance to influenza virus impetus the demands for new alternative antivirus substance, especially from nature products and traditional Chinese medicine (TCM) [7].

Acute lung injury (ALI) is characterized by severe lung edema and inflammation, and the pathogenesis of ALI involves immune imbalance [8]. Acute lung injury is the most common form of influenza A virus infection, during which the host alveolar epithelial cells are infected and injured [9]. When the host is infected, the virus can induce a series of signaling cascades to their own benefit, such as toll-like receptors (TLRs) and other signaling pathways [10]. As we all know, pathogen-associated molecular pattern (PAMP), as well as damage-associated molecular pattern (DAMP) activate antigen-presenting cells through TLRs to initiate immune responses [11]. DAMPs such as high mobility group box-1 protein (HMGB-1) are released early from the infected host cells in the extracellular medium in response to viral stimuli. Influenza virus infection can increase the expression of TLR4 in lung [12]. HMGB-1 is detected by TLR4 and leads to amplify inflammation and exacerbate tissue injury [13]. The binding of HMGB-1 to TLR4, as well as the recruitment of neutrophils to the infected areas accelerated the production of large amounts of oxidative products and proinflammatory cytokines, and further aggravated lung injury [14]. Influenza virus infection and COVID-19 both result in respiratory system damage and perhaps share similar infection process. Besides pneumonia and acute lung injury, other vital organs injury, such as liver, thymus, spleen, heart or kidneys dysfunction were observed in patient suffered from COVID-19 [15].

Traditional Chinese medicine, the precious treasure of China which stem from antique Chinese culture 2000 years ago, are used to treat diseases in China and southeast Asia. TCM played an significant role in the treatment of COVID-19, bringing new hope for the prevention and control of COVID-19 and influenza virus [16].

Indigo naturalis, a dark blue powder, mass or granules, is prepared from stems and leaves of *Baphicacanthus cusia* (Nees) Bremek. (Fam. Acanthaceae)*, Polygonum tinctorium* Ait. (Fam. Polygonaceae) *or Isatis indigotica* Fort. (Fam Cruciferae) [17, 18]. Indigo naturalis (Qingdai) is among the family of the traditional Chinses medicine with heat-clearing and detoxifying capacity. Indigo naturalis as a folk traditional Chinese medicine is used to treat psoriasis, colitis and upper respiratory system diseases [19]. Jinmo Shi, the famous doctor of traditional Chinese medicine used indigo naturalis to treat parotitis, acute and cholic pharyngitis and armydalitis [20].

Researchers have confirmed the definite effect of indigo naturalis on psoriasis and colitis, and the mechanisms of action has also been studied [21]. Indigo naturalis reduced the expression of cytokines and chemokines and inhibited the proliferation of keratinocytes and endothelial cells to treat psoriasis [22]. However, there are few reports on the effects and mechanisms of indigo naturalis on respiratory virus infection. In this experiment, a mouse model of IAV infection was established to study the effects and mechanisms of indigo naturalis on IAV-induced ALI.

Methods

Reagent

The powdered form of indigo naturalis was prepared from the leaves of *B. cusia* (Nees) Bremek and purchased from Shanghai Ley's Pharmaceutical Co., Ltd., with the place of production of xianyou county, Fujian province, China. The material was identified the authors. The voucher specimen of indigo naturalis (DFC-IN-201509) was deposited in Department of Natural Medicine, School of Pharmacy, Fudan University.

Ribavirin was purchased from Shanghai Meryer chemical Co., Ltd.. ELISA kits for mouse tumor necrosis factor-α (TNF-α), interleukin-6 (IL-6), monocyte chemoattractant protein-1 (MCP-1), regulated upon activation normal T cell expressed and secreted factor (RANTES), interleukin-10 (IL-10), and interferon induced protein-10 (IP-10) were purchased from Shanghai Boatman Biotechnology Co. Ltd.. ELISA kits for interferon-α (IFN-α), interferon β (IFN-β), interferon γ (IFN-γ), myeloperoxidase (MPO), methylene dioxyamphetamine (MDA) were purchased from Shanghai Beyotime Biotechnology Co., Ltd.. The anti-HMGB-1 and anti-TLR4 antibodies were purchased from Abcam (San Francisco, CA, USA). Alanine transaminase (ALT) and aspartate aminotransferase (AST) were determined using Roche Cobas 6000 c501 Chemistry Analyzer (Roche Diagnostics, Mannheim, Germany) and related reagents.

Herbal extract preparation

The indigo naturalis powder (2 kg) were packaged with 4 layers of etamine, and then extracted with boiling water for 1 h with three times. The water extract was concentrated under reduced pressure and lyophilized to produce 82 g of aqueous extract of indigo naturalis (INAE).

Chemical components identification from INAE

Analysis was performed using an UPLC-IT/MS system (Thermo, Finnigan, San Jose, CA, USA). Three milliliter of deionized water was added into 3 mg of powdered INAE, after vortex and sonication, the 1 mL/mg INAE stock solution was filtered through a 0.22 μm filter (Millipore) before injected to the UPLC-IT/MS analysis.

A YMC-Triart C_{18} column (150 × 2.1 mm i.d., 1.9μm; YMC, Japan) was used for sample preparation, with an injection volume of 5 μL for the constituent separation and analysis on the Dionex Ultimate-3000 UPLC-IT/MS Velos Pro ion-trap mass spectrometer system equipped with electrospray ionization source

in positive ion mode. The mobile phases consisted of water (A) and acetonitrile (B) at a flow rate of 0.3 mL/min. The MS parameters were optimized as follows: selections of the target mass range *m/z* of 110 ~ 2000; compound stability 100%; trap drive level 100%; collision energy 1V; auxiliary gas (N_2) flow rate of 10 L/min; the capillary temperature of 350°C; dry gas 8 L/min; capillary voltage of 30V; sheath gas (N_2) flow rate of 15 L/min; and nebulizer gas 40 psi were made by examination of the full grade scan intensity, stability, and the product ions spectra.

In vitro antiviral evaluation

The influenza A virus (H1N1 A/FM/1/47) was denoted by vice professor Haiyan Zhu, department of microbiological and biochemical pharmacy, school of pharmacy, Fudan University. According to the reference and procedures in our lab, the virus was suspended in Dulbecco's modified Eagle's medium (DMEM), propagated in lung of mice and stored at -80°C. The 50% lethal dose (LD_{50}) of virus was determined in mice infected with serial dilutions of virus [23].

Once attaching to host cells, virus propagate in and release virions from the infected host cells [24]. *In vitro* antiviral evaluation was conducted as described with minor modification [25]. Madin-Darby canine kidney (MDCK) cells were cultured in DMEM supplemented with 10% fetal bovine serum (Hyclone, CA, USA), streptomycin and penicillin. Briefly, MDCK cells were cultured in 96-well plates (1×10^5 cells per well) till cells fulfilled 90% percent of the bottom. INAE were diluted and prepared in concentrations of 0, 10, 25, 50, 100, 200 and 400 μg/mL. The antiviral process was investigated based on three ways of action: added the drugs 2 h prior to, incubated the drugs with 100 $TCID_{50}$ influenza A virus, or 2 h after virus infection. The cells with only infection virus were served as virus control. After 3-day's incubation, 3-(4,5-dimethyl-2-thiazolyl)-2,5-diphenyl-2-H-tetrazolium bromide (MTT) was added into the wells. Following 4 h incubation, the optical density value (OD value) of supernatant was tested. Inhibition rate (%) = [(OD of INAE – mean OD of virus control) / (mean OD of cells control – mean OD of virus control)] × 100%.

In vitro anti-inflammatory effect

BALB/c mice were administrated with 5% mercaptoethanol acid sodium by intra-peritoneal injection and scarified 4 days later to harvest peritoneal macrophages. Macrophages were suspended with RPMI-1640 culture medium containing 10% fetal bovine serum and antibiotics. The cells were cultured in 96 cell plate (1×10^6 cells per well) for 2 h. The serial dilutions of INAE, lipopolysaccharide (LPS, 1 μg/ml), and dexamethasone (positive control, 10 μM) were added and incubated for 24 h. A sample of cells without LPS was set aside to serve as a control. The supernatant was collected at the end of the incubation. The nitrogen oxide (NO) concentration in the supernatant was calculated by measuring the OD value of supernatant following the instruction of method using Griess reagent [26].

Animals

Specific pathogen-free male BALB/c mice (14 ~ 16 g) were purchased from Shanghai SLAC Laboratory Animal Co., Ltd. [SCXK (Hu) 2012-0002]. The mice were housed in collective cages under a 12 h light/dark

room, with free access to food and water. The air temperature was maintained at 22 ± 2°C with relative humidity of 50 ± 10%. Experiments were carried out according to the guideline for the care of laboratory animals of national institutes of health. All study protocols were approved by the animal ethical committee of school of pharmacy, Fudan University (approval No. 2015-10-SY-CDF-01).

Survival experiment

Survival experiment is the usual and important experiment to evaluate the effects of compound on reducing the lethality of IAV infection [3]. The survival experiment was conducted as described with minor modification [27]. Mice were randomly divided into six groups (n = 10): normal, model, INAE (40, 80 and 160 mg/kg) and positive control (ribavirin, 100 mg/kg). Mice were anaesthetized by tail intravenous injection of propofol (0.026 mL/10g) and were intranasal challenged with 6 × LD_{50} IAV in 30 μL RPMI-1640 medium 2 h before the compound treatment. Normal mice were challenged with 30 μL RPMI-1640 medium. The mice were treated orally with INAE or ribavirin once daily for 7 days. For comparison, normal group and model group were given 0.5% carboxymethyl cellulose sodium (CMC-Na). All groups were monitored for 14 days after virus infection. Body weight, body temperature, and animal clinical health were monitored daily. Lifespan and mortality rate of mice were calculated.

Acute lung injury experiment

In order to study the efficacy and mechanisms of INAE on IAV infection, acute lung injury in mice was induced by IAV infection in a 4-day experiment [8]. The experiment was scheduled by six groups (n = 6): normal, model, INAE (40, 80 and 160 mg/kg) and positive control (ribavirin, 100 mg/kg). Mice were challenged with 3 × LD_{50} IAV in 30 μL RPMI-1640 medium 2 h before the compound treatment. Normal mice were challenged with 30 μL RPMI-1640 medium. The mice were orally treated with agents as we mentioned about. The treatment began 2 h after the virus challenge and once daily for 4 days. The mice were sacrificed on the 4^{th} day after virus infection. The lung tissues were harvested, weighted and then washed with pre-chilled saline. The superior right lobe was cut and placed in 10% neutral formalin buffer for histopathologic evaluation, and the rest parts were snap frozen at -80°C for cytokine detection. To estimate the severity of lung, liver, thymus and spleen, organ indexes were calculated as follows: Organs index = Organ weight (mg) / body weight (g) × 100%. Serum ALT and AST levels were also detected to evaluate the severity of liver injury.

Lung tissues were fixed in 10% neutral formalin buffer. After fixation, the samples were dehydrated and embedded in paraffin. The embedded samples were cut into 5-μm slices and stained with hematoxylin and eosin (H&E). Lesions in lung were observed by optical microscopy. Lung injury were determined through the severity of pneumonia in a blinded fashion [27].

After rehydrated through a graded series of alcohol, the slices were incubated with rabbit antibodies against HMGB-1 (1:200 diluted) and TLR4 (1:250 diluted) at 4°C overnight. The sections were then incubated with special HRP-conjugated goat anti-rabbit IgG antibody at 37°C for 30 minutes. Slides were

stained with chromogenic substrate solution diaminobezidin (DAB) and counterstained with hematoxylin. The expression of HMGB-1 and TLR4 were visualized under a microscope [28]. The expression of HMGB-1 and TLR4 were also assessed by semi-quantitative analysis using ImageJ software.

Determination of lung virus titer

The frozen lung tissues were thawed and homogenized in PBS at a concentration of 100 mg tissue/1 mL PBS as described with minor modification [29]. The supernatant was split into aliquots and stored at -80°C for subsequent use.

MDCK cells were plated at 2×10^6 cells in 96 cell plate till the cells grown to 90% confluent, cells were then infected with serial dilutions of supernatant from lung homogenate and incubated for 2 h at 37°C with 5% CO_2. The supernatant was removed and the wells were washed with PBS and incubated with 200 µL DMEM at 37°C, 5% CO_2 for 3 days. The cell activity was assessed by MTT assays. The lung virus titer was expressed by the inhibition rate of virus replication [30].

Anti-oxidant capacity in supernatant of lung homogenate

The anti-oxidation capacity of INAE was tested through method of ferric ion reducing antioxidant power (FRAP). Levels of MPO and MDA, the oxidant stress products in lung homogenate of IAV infected mice were also evaluated by detection kits according to the manufacturer's instructions.

Assessment of cytokines in supernatant of lung homogenate

Levels of IFN-α, IFN-β, IFN-γ, MCP-1, RANTES, IP-10, TNF-α, IL-6, and IL-10 in lung homogenate of IAV-infected mice were determined with ELISA kits according to the manufacturer's instructions.

1. ## Statistical analysis

All parameters were recorded for individuals within all groups and statistical computations were performed with GraphPad prism 6 (GraphPad software Inc., San Diego, CA, USA). Data comparison were carried out with one-way ANOVA and expressed as mean ± S.D. (Standard deviation). Post hoc comparisons were performed using Fishers's PLSD if any significant changes were found. The *P* values less than 0.05 were considered as statistically significant.

Results

Chemical components identification from INEA

The chemical components of INAE was identified by UPLC-ESI-LTQ-MS analysis system. Positive mode chromatography was chosen to characterize the chemical constituents for more plentiful chromatographic peaks were detected in positive mode than in negative mode. According to the well-known phytochemical compounds from indigo naturalis, chemical name, MS^1 data, fragment of MS^2

data, retention times and *m/z* values of the molecular ions, 16 chemicals were identified from INAE as Tab. 1 and Fig.1: 9 alkaloids, 3 nucleosides, 1 terpene, 2 amino acid and 1 original acid.

Anti-influenza and anti-inflammatory effects of INAE *in vitro*

The result showed that INAE had no toxicity on MDCK cells up to concentration of 1000 μg/mL (data not shown). As shown in Fig. 2A, INAE was administrated 2 h prior to virus infection (to interfere the adhesion process of virus to cells), the inhibition rate of virus replication gradually increased up to 60% as compound concentration increased to 400 μg/mL). No obvious inhibition was observed on the cells treated with virus mix-incubated INAE simultaneously (direct killing effect of INAE to virus) or with INAE 2 h after virus infection (to interfere the release of virion from cells). The result demonstrated that INAE inhibited the process of adhesion of virus to cells, but had no direct killing effect to virus *in vitro*.

As shown in Fig. 2B, compared with cell control group, LPS stimulation significantly increased NO production in peritoneal macrophages. INAE administration (17, 34 and 68 μg/mL) remarkable suppressed the elevated NO production induced by LPS ($P < 0.05$).

inAE improved lifespan and survival rate of IAV-infected mice

The mice infected with IAV were observed for 14 days. The mice showed clinical signs of piloerection, ruffled fur, lack of food consumption, and body weight loss after virus inoculation. INAE significantly expanded the lifespan of IAV-infected mice (Fig.3A). Model group mice had a notable low survival time (8.30 ± 0.67 days) compared with INAE groups mice (ranged from 9.80 ± 2.12 days to 10.80 ± 2.66 days).

There was no death in normal group during 14-day's observation. Mice in model group were found dead since the 7^{th} day after IAV infection and 100% of the model mice died within 9 days (Fig.3B). The survival rate of mice in model group was 0% since the 9^{th} day. Mice treated with INAE (40, 80 and 160 mg/kg) were protected from lethality. When compared with model group, the survival rate of mice significantly raised in INAE 40 and 80 mg/kg groups during days 8 ~ 9 ($P < 0.05$), and in INAE 160 mg/kg group during days 8 ~ 12 ($P < 0.05$). The survival rate of INSE (40, 80 and 160 mg/kg) on the 14^{th} day were 10%, 10%, and 20%.

Animal body temperature was also reported during the study. It is worth noting that the body temperature of mice in model group was notably lower than normal group, while INAE treatment groups exhibited higher temperature than model group during the study (Fig.3C).

INAE alleviated IAV-induced acute lung injury

INAE was administrated to evaluate the effect on IAV-induced ALI. Significant body weight loss and lung index increase were exhibited in mice infected with IAV. As shown in Fig.4C, IAV infected mice began to lose body weight since the 2^{nd} day after IAV infection. Compared with model group, body weight of mice treated with INAE and ribavirin were significantly higher on the 3^{rd} day and the 4^{th} day ($P < 0.05$). Compared with normal group (6.26 ± 0.36), remarkable increase of lung index was observed in

model group (10.78 ± 0.93 mg/g). Comparatively, treatment with INAE (Fig.4B) significant decreased the lung index (80 mg/kg, 9.25 ± 1.39 mg/g; 160 mg/kg, 8.34 ± 0.72 mg/g).

Pathologic findings indicated that normal group mice had lungs in terms of nature size, color, and texture with clear and intact round alveolar cells (Fig.4A). In the contrary, large areas of alveolar cells and bronchioles were damaged and most alveolar walls were destroyed in model group. Amounts of inflammatory cells infiltration was observed in injured alveolus and pneumocytes drop off from bronchiole. Histological damages in lung of mice were obviously alleviated in INAE treated groups. Inflammatory cell infiltration was significantly decreased compared with model group.

INAE lowered virus titer in lung of IAV-infected mice

Acute lung injury referred to virus replication and virus titer were determined by $TCID_{50}$. As shown in Fig.4D, virus titer in lung homogenate of mice treated with INAE (40 mg/kg, 3.78 ± 0.15; 80 mg/kg, 3.50 ± 0.20; 160 mg/kg, 2.87 ± 0.12) and ribavirin (2.36 ± 0.14) were clearly lower than that of model group (4.78 ± 0.16) on the 4^{th} day after IAV infection ($P < 0.05$). The result suggested that the decrease of virus titer was accordance with the protective effect of INAE on lung injury.

INAE reduced injury in liver, thymus and spleen

As shown in Fig. 5A and 5B, weights of liver, thymus and spleen of mice in model group were significantly decreased compared with normal group ($P < 0.05$). Comparatively, INAE administration (40, 80 and 160 mg/kg) significant increased weights and organ index of liver, and administration of 160 mg/kg of INAE significantly increased both weight, organ indexes of thymus and spleen.

Serum ALT and AST are the main predictor of liver injury [31]. As shown in Fig. 5C, serum ALT and AST levels increased significantly in model group compared with normal group ($P < 0.05$). INAE administration significantly decreased ALT (40, 80 and 160 mg/kg) and AST (and 160 mg/kg) levels compared with model group ($P < 0.05$).

INAE suppressed the expression of HMGB-1 and TLR4 in lung of IAV-infected mice

As shown in Fig.6A, mice in normal group basically expressed HMGB-1 in nuclei of lung tissue. Compared with normal group, the expression of HMGB-1 in model group increased and a large amount of HMGB-1 was found out of nuclei and cells. INAE and ribavirin reduced the over expression and the release of HMGB-1. Mice in normal group expressed a small quantity TLR4, while the expression increased in model group. Immunohistochemistry staining of HMGB-1 and TLR4 were also assessed by semi-quantitative analysis using ImageJ software (Fig.6B). Compared with model group, the expression of HMGB-1 and TLR4 were significantly decreased ($P < 0.05$) as the concentration of compound increased.

INAE increased anti-oxidant capacity and inhibited oxidant stress

As shown in Fig.7, the FARP value in lung homogenate of mice in model group significantly decreased compared with that in normal group ($P < 0.05$). INAE administration significantly increased the FARP value compared with model group ($P < 0.05$). The levels of MPO and MDA in lung homogenate significantly increased in model group compared with normal group ($P < 0.05$). In comparison with model group, INAE administration markedly reduced production of MPO and MDA ($P < 0.05$). The decrease of production of MPO and MDA demonstrated the remarkable anti-oxidant capacity of INAE.

INAE inhibited inflammatory response in lung of IAV-infected mice

As shown in Fig.8, the levels of IFN-α, IFN-β in lung homogenate significantly increased in model group compared with normal group ($P < 0.05$). In comparison with model group, INAE administration significantly reduced IFN-α and IFN-β expression ($P < 0.05$). The level of IFN-γ significantly decreased in model group and INAE administration significantly increased IFN-γ expression ($P < 0.05$).

In comparison with normal group, model group exhibited significant increase in levels of chemokines MCP-1, RANTES and IP-10 ($P < 0.05$). Treatment with INAE significantly decrease the expression of MCP-1, RANTES and IP-10 ($P < 0.05$) in lung homogenate of IAV-infected mice.

Moreover, the expression of TNF-α and IL-6 in lung homogenate of mice in model group significantly increased compared with normal group ($P < 0.05$). INAE administration markedly reduced the expression of TNF-α and IL-6 ($P < 0.05$). IL-10 is an important anti-inflammatory factor that can ameliorate immunopathology by limiting immune responses involved in tissue damage. The expression of IL-10 significantly decreased in lung homogenate of mice in model group compared with normal group ($P < 0.05$). The administration of INAE significantly increased IL-10 production in lung homogenate of IAV-infected mice ($P < 0.05$).

Discussion

Traditional Chinese medicine is effective in prevention and enhancing the resistance to pandemic with unique insights [32]. Many traditional Chinese herbs, for instance, *Radix isatidis* (Banlangen), *Houttuynia cordata* (Yuxingcao), *Radix Scutellariae* (Huangqin), *Folium isatidis* (Daqingye) were proved to exhibit anti-virus effect during pandemics of SARS in 2003 [33-35]. During the treatment period of COVID-19, TCM scheme was included in the guideline on diagnosis and treatment of COVID-19, and TCM fully participate in the whole rescue process [36]. Decoction is the main form of TCM [37]. Yin-Ku Lin *et al.* found that the abstracts of indigo naturalis in oil reduced nail psoriasis severity index in patient, and the abstracts of indigo naturalis in dimethyl sulfoxide suppressed the increase of protein carbonyl groups in human keratinocytes [38, 39]. However, as the main therapeutic dosage form of TCM, there are few researches regarding the effect of indigo naturalis on IAV-induce ALI. In our study, INAE as the aqueous extract of indigo naturalis was studied referred to clinical use of TCM.

After herbal extract preparation, the constituents of INAE was analyzed using an UPLC-ESI-LTQ-MS system. In the experiment, more plentiful chromatographic peaks were detected in positive mode than in

negative mode, and positive mode was chosen to characterize the chemical constituents of INAE. According to the retention times and *m/z* values of the molecular ions, 16 chemicals, including 9 alkaloids, 3 nucleosides, 2 amino acids, 1 terpene and 1 organic acid, were identified through the comparison with the standard compounds and the database of known chemicals. Among these chemicals, alkaloids were the main small molecule in indigo naturalis [40, 41]. Alkaloids has been proven to exhibit antiviral efficacy and inhibit LPS induced inflammation [42, 43].

The process of virus infection to host cells has three different phases：attachment of virus to host cells, virus replication in and release of virion from host cells [24]. The anti-influenza effect of INAE was evaluated *in vitro* first. INAE were inoculated 2 h prior to, simultaneously, or 2 h after IAV infection with MDCK cells to test the ani-virus efficacy in three different phases. *In vitro* results shown that INAE markedly inhibited virus adhesion to cells when administrated before virus infection, but had no inhibitive effect on virus replication and release.

In our study, INAE suppressed the elevated NO production from LPS-stimulated peritoneal macrophages *in vivo.* NO produced by iNOS is an important proinflammatory mediator. NO has direct antiviral properties against some viruses, whereas during virus infections NO can mediate immunopathology and/or inhibit the antiviral immune response to promote chronic infection [44]. Accumulated evidence suggests that NO and oxygen radicals such as superoxide are key molecules in the pathogenesis of various infectious diseases and accelerate tissue damage [45]. Free radical such as NO is highly active chemical substances which is exceptionally destructive, indiscriminately causing protein deterioration, cell membrane destruction, DNA damage, cell death, and organ failure [46]. It is known that virus infection induces massive production of free radicals [47]. Most cytokines, such as IFN-γ, IL-1β, IL-2, IL-6, TNFα can all stimulate the generation of NO [48]. Inhibition of NO synthesis can decrease the production of IL-6 and the cytotoxicity effect of inflammatory cytokines can be blocked by lipid peroxidation inhibitor [49]. Mice deficient in inducible NO synthase exhibited reduced morbidity and mortality when challenged with influenza virus, which told us that NO is the culprits in the virus induced pneumonia death [50]. The *in vitro* effect of INAE on inhibiting the over production of NO might be helpful for reducing the production of inflammatory cytokines and oxidative tissue damage in IAV-infected mice.

In our study, treatment with INAE significantly expanded the lifespan and increased the survival rate of IAV-infected mice. Oral administration of INAE significant alleviated lung injury with reduced lung index and virus titer, as well as decreased inflammatory cells infiltration in lung. Our study results that can alleviate acute lung injury is accordance with clinic treatment [20]

The model of acute lung injury induced by IAV is usually used for research of anti-influenza agents. Once mice were infected with IAV, amounts of influenza virus infecting pneumocytes results in cells necrosis and apoptosis in lung tissues and causes acute lung injury [51]. Disorder of balance between inflammation and anti-inflammation led to death of mice for the reason of continuous injury of lung and other organs [52]. In our study, severe injury of vital organs, including lung, liver, thymus and spleen were observed in IAV-infected mice. Administration of INAE alleviated injury of vital organs, especially

decreased lung weight and lung index. The liver weight and index, the serum ALT and AST production were also reduced by INAE treatment. Spleen and thymus injury were also released in high group of INAE administration. Like influenza virus infection, liver demonstrated diffuse mononuclear and hepatic necrosis, and splenic tissue were shown to be atrophic in the current outbreak of COVID-19 infected patient [53, 54]. Most of the recommended prescriptions consists TCM, which have the efficacy of heat-clearing and detoxicating. Indigo naturalis also has the similar feature, which provide a possibility that INAE might make contribution to attenuate multi organ failure in COVID-19 and more researches are needed for further discovery [55, 56].

During the process of virus infection, amounts of HMGB-1 were released into the infected tissues due to tissue injury [57]. HMGB-1 was implicated in host tissue destruction and persistent pathological changes in IAV-infected hosts [58]. HMGB-1 is a crucial mediator in the pathogenesis of several viral infections, it can be released passively from necrotic cells and/or actively secreted by macrophages or monocytes into the extracellular milieu [59]. As a ligand of TLR4, HMGB-1 can activate alveolar macrophages to produce proinflammatory cytokines and induce ALI [60, 61]. TLR4, one of the important inflammatory signal receptors of the pathogen recognition receptors family (PRR), plays a critical role in the activation of immune system as influenza virus and COVID-19 invasion [62, 63]. TLR4 is also an important transmembrane protein for the development of cytokines production [64]. There is growing evidence that TLR4 signal inhibition alleviated lung injury in IVA infected mice [65, 66]. Our experiment demonstrated that INAE obviously inhibited over expression of HMGB-1 and TLR4 that might benefit the alleviation of lung injury in IAV infected mice.

Some cases showed neutrophil infiltration contributed to cytokine storm in virus infection [53]. FRAP is a global indicator of antioxidant capacity [67]. MPO is an enzyme mainly found in azurophilic granules of neutrophils, which serves as a good marker of inflammation, tissue injury and neutrophil infiltration [68]. Oxidative damage may represent crucial pathogenic factor in acute lung injury due to the increased production of reactive oxygen and nitrogen species [69]. MDA is the main products of lipid peroxidation and mediate inflammation [70]. Treatment with INAE increased FRAP, and decreased MPO, MDA production in lung homogenate of IAV-infected mice, which demonstrated that INAE increased anti-oxidant capacity and suppressed oxidant stress.

Excessive production of proinflammatory factors plays a critical role in the pathogenesis of influenza virus infection. Lung damage and clinic symptoms associated with aberrant and uncontrolled cytokine production could ultimately lead to death [71]. TNF-α and IL-6 were the early immune cytokines contribute to the proinflammatory production [72]. Chemokines then give the signal for the directed migration of neutrophils or macrophages into the tissues. MCP-1 and RANTES are the main chemokines during early infection stage of influenza [8, 73]. IP-10 belongs to the chemokine CXC subfamily and acts as a chemo attractor for T cells and NK cells. IL-10 is a critical protective modulator which can attenuate the activation of lymphocytes and inflammatory cascades during virus infection. Importantly, a research demonstrated that induction of IP-10 in lung attracted pulmonary neutrophils, and led to lung inflammation during influenza infection [74]. Increasing IP-10 induction was consistently found in the

serum of H5N1-infected patients and animal models [75]. The present study demonstrated that treatment with INAE remarkable modulated levels of antivirus factors (IFN-α, IFN-β and IFN-γ), decreased levels of chemokines MCP-1, RANTES and IP-10, and reduced the production of proinflammatory factors TNF-α and IL-6. Meanwhile, INAE significantly increased the production of anti-inflammatory factor (IL-10). It is all known that the aggressive pro-inflammatory response and insufficient control of anti-inflammatory response in virus infection such as influenza infection, SARS and COVID-19, lead to systemic cytokine storm and accelerate tissue injury [53]. Our study demonstrated the inhibition effects of INAE on cytokines and chemokines, oxidant production, and suppression of neutrophilia infiltration (reflected by MPO level in Fig 7). Based on the beneficial effect of INAE, we supposed that INAE might reduce the risk of cytokine storm in severe virus infection.

Our research studied the anti-inflammatory and antiviral effects of indigo naturalis both *in vivo* and *in vitro*. INAE inhibited the adhesion process of virus to host cell *in vitro* to reduced virus replication, but had no direct killing effect on virus. *In vivo* experiment showed INAE treatment extended the lifespan and reduced the mortality of IAV-infected mice, and reduced virus titer in lung tissue, which demonstrated the antiviral effect of INAE *in vivo*. On the other hand, INAE inhibited the production of NO induced by LPS, showing an anti-inflammatory effect *in vitro*. *In vivo* experiments showed that INAE inhibited the HMGB-1 and TLR4 signaling pathway, reduced the extensive production of pro-inflammatory cytokines and chemokines, as well as the tissue-damaging peroxide products. The multi-targets effects of INAE contributed to improve the lung injury caused by influenza virus infection.

Conclusion

In summary, our investigation described the beneficial effect of indigo naturalis against ALI in IAV infected mice, and the underlying mechanism might be closely associated with its inhibition of virus replication, anti-inflammatory and anti-oxidant effects (Fig. 9). As acute lung injury, multi organ failure such as liver, thymus and spleen, and cytokine storm occurred both in influenza virus and SARS-CoV-2 infection, our study suggested indigo naturalis could be a promising agent and warrant further evaluation for treatment of influenza A virus induced acute lung injury and SARS-CoV-2 induced COVID-19.

Abbreviations

INAE: Aqueous extract of indigo naturalis; ALI: Acute lung injury; IAV: Influenza A virus; COVID-19: Coronavirus disease 19; SARS-CoV-2: Severe acute respiratory coronavirus 2; PAMP: Pathogen-associated molecular pattern; DAMP: Damage-associated molecular pattern; PRR: Pathogen recognition receptors; HMGB-1: High mobility group box-1 protein; TLR4: Toll-like receptor 4; TCM: Traditional Chinese medicine; LD_{50}: 50% of lethal dose; MDCK: Madin-Darby canine kidney; DMEM: Dulbecco's modified Eagle's medium; MTT: 3-(4,5-dimethyl-2-thiazolyl)-2,5-diphenyl-2-H-tetrazolium bromide; OD: Optical density; CMC-Na: Carboxymethyl cellulose sodium; DAB: Diaminobezidin; IFN-α: Interferon α; IFN-β: Interferon β; IFN-γ: Interferon γ; MCP-1: Monocyte chemoattractant protein-1; RANTES: Regulated upon activation normal T cell expressed and secreted factor; IP-10: Interferon induced protein-10; TNF-α: Tumor necrosis

factor-α; IL-6: Interleukin-6; IL-10: Interleukin-10; FRAP: Ferric ion reducing antioxidant power; MPO: Myeloperoxidase; MDA: Malonaldehyde; NO: Nitrogen oxide; LPS: lipopolysaccharide; H&E: Hematoxylin and eosin; ANOVA: One-way analysis of variance; S.D.: Standard deviation.

Declarations

Acknowledgements

Not applicable.

Authors' contribution

Daofeng Chen conceived and designed the work. Hong Li, Yunyi Zhang, Yan Lu and Haiyan Zhu contributed to study design of immunology, antivirus and chemistry, and development of the study protocol. Rong Tian contributed to the chemistry analysis. Lijun Ling contributed to *in vivo* experiment. Peng Tu takes responsibility for the integrity of the work as a whole, from inception to publication. All authors had read and approved the submitted version of the manuscript.

Funding

This work was supported by the National Key R&D Program of China (grant No. 2019YFC 1711000) and the National Natural Science Foundation of China (grant No.81330089).

Availability of data and materials

The datasets used and/or analyzed during the current study are available from the corresponding author on reasonable request.

Ethics approval and consent to participate

The study on animal was approved by the animal ethical committee of school of pharmacy, Fudan University (approval No. 2015-10-SY-CDF-01).

Consent for publication

Not applicable.

Competing interests

The authors declare that there are no conflicts of interest regarding the publication of this article.

Author details

1. Department of Natural Medicine, School of Pharmacy, Fudan University, Shanghai, 201203, P. R. China

2. Department of Pharmacology, School of Pharmacy, Fudan University, Shanghai, 201203, P. R. China

3. Department of Microbiological and Biochemical Pharmacy, School of Pharmacy, Fudan University, Shanghai, 201203, P. R. China

References

[1] Li K, Hao Z, Zhao X*, et al.* SARS-CoV-2 infection-induced immune responses: Friends or foes? [J]. *Scand J Immunol*, 2020: e12895.

[2] Goldstein JL. The Spanish 1918 Flu and the COVID-19 Disease: The Art of Remembering and Foreshadowing Pandemics [J]. Cell, 2020, 183(2): 285-289.

[3] Ling LJ, Lu Y, Zhang YY*, et al.* Flavonoids from Houttuynia cordata attenuate H1N1-induced acute lung injury in mice via inhibition of influenza virus and Toll-like receptor signalling [J]. *Phytomedicine*, 2020, **67**: 153150.

[4] Zhi H, Jin X, Zhu H*, et al.* Exploring the effective materials of flavonoids-enriched extract from Scutellaria baicalensis roots based on the metabolic activation in influenza A virus induced acute lung injury [J]. *J Pharm Biomed Anal*, 2020, **177**: 112876.

[5] Lo CY, Tang YS and Shaw PC. Structure and Function of Influenza Virus Ribonucleoprotein [J]. *Subcell Biochem*, 2018, **88**: 95-128.

[6] Pizzorno A, Padey B, Terrier O*, et al.* Drug Repurposing Approaches for the Treatment of Influenza Viral Infection: Reviving Old Drugs to Fight Against a Long-Lived Enemy [J]. *Front Immunol*, 2019, **10**: 531.

[7] Fu YJ, Yan YQ, Qin HQ*, et al.* Effects of different principles of Traditional Chinese Medicine treatment on TLR7/NF-kappaB signaling pathway in influenza virus infected mice [J]. *Chin Med*, 2018, **13**: 42.

[8] Zhi HJ, Zhu HY, Zhang YY*, et al.* In vivo effect of quantified flavonoids-enriched extract of Scutellaria baicalensis root on acute lung injury induced by influenza A virus [J]. *Phytomedicine*, 2019, **57**: 105-116.

[9] Short KR, Kasper J, van der Aa S*, et al.* Influenza virus damages the alveolar barrier by disrupting epithelial cell tight junctions [J]. *Eur Respir J*, 2016, **47**(3): 954-966.

[10] Ma Q, Huang W, Zhao J*, et al.* Liu Shen Wan inhibits influenza a virus and excessive virus-induced inflammatory response via suppression of TLR4/NF-kappaB signaling pathway in vitro and in vivo [J]. *J*

Ethnopharmacol, 2020, **252**: 112584.

[11] Senthilkumar D, Rajukumar K, Kumar M*, et al.* Porcine reproductive and respiratory syndrome virus induces concurrent elevation of High Mobility Group Box-1 protein and pro-inflammatory cytokines in experimentally infected piglets [J]. *Cytokine*, 2019, **113**: 21-30.

[12] He J, Yuan R, Cui X*, et al.* Anemoside B4 protects against Klebsiella pneumoniae- and influenza virus FM1-induced pneumonia via the TLR4/Myd88 signaling pathway in mice [J]. *Chin Med*, 2020, **15**: 68.

[13] Doganyigit Z, Okan A, Kaymak E*, et al.* Investigation of protective effects of apilarnil against lipopolysaccharide induced liver injury in rats via TLR 4/ HMGB-1/ NF-kappaB pathway [J]. *Biomed Pharmacother*, 2020, **125**: 109967.

[14] Sun Y, Su J, Liu Z*, et al.* Aflatoxin B1 Promotes Influenza Replication and Increases Virus Related Lung Damage via Activation of TLR4 Signaling [J]. *Front Immunol*, 2018, **9**: 2297.

[15] Garg S, Garg M, Prabhakar N*, et al.* Unraveling the mystery of Covid-19 cytokine storm: From skin to organ systems [J]. *Dermatol Ther*, 2020: e13859.

[16] Ren JL, Zhang AH and Wang XJ. Traditional Chinese medicine for COVID-19 treatment [J]. *Pharmacol Res*, 2020, **155**: 104743.

[17] Commission CP. Chinese pharmacopoeia [J]. *China Medical Science Press, Beijing*, 2010, **228**.

[18] Hsieh W-L, Lin Y-K, Tsai C-N*, et al.* Indirubin, an acting component of indigo naturalis, inhibits EGFR activation and EGF-induced CDC25B gene expression in epidermal keratinocytes [J]. *Journal of dermatological science*, 2012, **67**(2): 140-146.

[19] Lin Y-K, Leu Y-L, Yang S-H*, et al.* Anti-psoriatic effects of indigo naturalis on the proliferation and differentiation of keratinocytes with indirubin as the active component [J]. *Journal of dermatological science*, 2009, **54**(3): 168-174.

[20] lǔ J. *Shijinmo variorum of clinic practices with double-herb prescriptions* [M]. People's Medical Publishing House, 2002.

[21] Naganuma M. Treatment with indigo naturalis for inflammatory bowel disease and other immune diseases [J]. *Immunol Med*, 2019, **42**(1): 16-21.

[22] Gu S, Xue Y, Gao Y*, et al.* Mechanisms of indigo naturalis on treating ulcerative colitis explored by GEO gene chips combined with network pharmacology and molecular docking [J]. *Sci Rep*, 2020, **10**(1): 15204.

[23] Lin SC, Kappes MA, Chen MC*, et al.* Distinct susceptibility and applicability of MDCK derivatives for influenza virus research [J]. *PLoS One*, 2017, **12**(2): e0172299.

[24] Konevtsova OV, Roshal DS, Losdorfer BoZic A*, et al.* Hidden symmetry of the anomalous bluetongue virus capsid and its role in the infection process [J]. *Soft Matter*, 2019, **15**(38): 7663-7671.

[25] Huang D, Peng WJ, Ye Q*, et al.* Serum-Free Suspension Culture of MDCK Cells for Production of Influenza H1N1 Vaccines [J]. *PLoS One*, 2015, **10**(11): e0141686.

[26] Larson KC, Lipko M, Dabrowski M*, et al.* Gng12 is a novel negative regulator of LPS-induced inflammation in the microglial cell line BV-2 [J]. *Inflamm Res*, 2010, **59**(1): 15-22.

[27] Zhu H, Lu X, Ling L*, et al.* Houttuynia cordata polysaccharides ameliorate pneumonia severity and intestinal injury in mice with influenza virus infection [J]. *J Ethnopharmacol*, 2018, **218**: 90-99.

[28] Xu YY, Zhang YY, Ou YY*, et al.* Houttuyniacordata Thunb. polysaccharides ameliorates lipopolysaccharide-induced acute lung injury in mice [J]. *J Ethnopharmacol*, 2015, **173**: 81-90.

[29] Hodgins B, Pillet S, Landry N*, et al.* Prime-pull vaccination with a plant-derived virus-like particle influenza vaccine elicits a broad immune response and protects aged mice from death and frailty after challenge [J]. *Immun Ageing*, 2019, **16**: 27.

[30] Thornton HV, Turner KME, Harrison S*, et al.* Assessing the potential of upper respiratory tract point-of-care testing: a systematic review of the prognostic significance of upper respiratory tract microbes [J]. *Clin Microbiol Infect*, 2019, **25**(11): 1339-1346.

[31] Zhang S, Hu B, Xu J*, et al.* Influenza A virus infection induces liver injury in mice [J]. *Microb Pathog*, 2019, **137**: 103736.

[32] Tong T, Wu YQ, Ni WJ*, et al.* The potential insights of Traditional Chinese Medicine on treatment of COVID-19 [J]. *Chin Med*, 2020, **15**: 51.

[33] Lau K-M, Lee K-M, Koon C-M*, et al.* Immunomodulatory and anti-SARS activities of Houttuynia cordata [J]. *Journal of ethnopharmacology*, 2008, **118**(1): 79-85.

[34] Lau T, Leung P, Wong E*, et al.* Using herbal medicine as a means of prevention experience during the SARS crisis [J]. *The American journal of Chinese medicine*, 2005, **33**(03): 345-356.

[35] Peng J, Fan G and Wu Y. Isolation and purification of clemastanin B and indigoticoside A from Radix Isatidis by high-speed counter-current chromatography [J]. *Journal of Chromatography A*, 2005, **1091**(1): 89-93.

[36] Wang J and Qi F. Traditional Chinese medicine to treat COVID-19: the importance of evidence-based research [J]. *Drug Discov Ther*, 2020, **14**(3): 149-150.

[37] Li K, Chen X, Zhong J*, et al.* The effects of the Xijiao Dihuang decoction combined with Yinqiao powder on miRNA-mRNA profiles in mice infected with influenza a virus [J]. *BMC Complement Med Ther*,

2020, **20**(1): 286.

[38] Lin YK, See LC, Huang YH*, et al.* Efficacy and safety of Indigo naturalis extract in oil (Lindioil) in treating nail psoriasis: a randomized, observer-blind, vehicle-controlled trial [J]. *Phytomedicine*, 2014, **21**(7): 1015-1020.

[39] Lin YK, Chen HW, Yang SH*, et al.* Protective effect of indigo naturalis extract against oxidative stress in cultured human keratinocytes [J]. *J Ethnopharmacol*, 2012, **139**(3): 893-896.

[40] Liu Z, Yang ZQ and Xiao H. Antiviral activity of the effective monomers from Folium Isatidis against influenza virus in vivo [J]. *Virol Sin*, 2010, **25**(6): 445-451.

[41] Lee CL, Wang CM, Hu HC, et al. Indole alkaloids indigodoles A-C from aerial parts of Strobilanthes cusia in the traditional Chinese medicine Qing Dai have anti-IL-17 properties [J]. Phytochemistry, 2019, 162: 39-46.

[42] Zhang M, Ding X, Kang J*, et al.* Marine Natural Product for Pesticide Candidate: Pulmonarin Alkaloids as Novel Antiviral and Anti-Phytopathogenic-Fungus Agents [J]. *J Agric Food Chem*, 2020, **68**(41): 11350-11357.

[43] Gao P, Wang L, Zhao L*, et al.* Anti-inflammatory quinoline alkaloids from the root bark of Dictamnus dasycarpus [J]. *Phytochemistry*, 2020, **172**: 112260.

[44] Kim M, Park KH and Kim YB. Identifying Active Compounds and Targets of Fritillariae thunbergii against Influenza-Associated Inflammation by Network Pharmacology Analysis and Molecular Docking [J]. *Molecules*, 2020, **25**(17).

[45] Yamashiro R, Misawa T and Sakudo A. Key role of singlet oxygen and peroxynitrite in viral RNA damage during virucidal effect of plasma torch on feline calicivirus [J]. *Sci Rep*, 2018, **8**(1): 17947.

[46] Abdul-Cader MS, Ahmed-Hassan H, Amarasinghe A*, et al.* Toll-like receptor (TLR)21 signalling-mediated antiviral response against avian influenza virus infection correlates with macrophage recruitment and nitric oxide production [J]. *J Gen Virol*, 2017, **98**(6): 1209-1223.

[47] El Sahly HM, Makedonas G, Corry D*, et al.* An evaluation of cytokine and cellular immune responses to heterologous prime-boost vaccination with influenza A/H7N7-A/H7N9 inactivated vaccine [J]. *Hum Vaccin Immunother*, 2020: 1-8.

[48] Yagmurdur H, Binnetoglu K, Astarci HM*, et al.* Propofol attenuates cytokine-mediated upregulation of expression of inducible nitric oxide synthase and apoptosis during regeneration post-partial hepatectomy [J]. *Acta Cir Bras*, 2017, **32**(5): 396-406.

[49] Adams C, Sawh F, Green-Johnson JM*, et al.* Characterization of casein-derived peptide bioactivity: Differential effects on angiotensin-converting enzyme inhibition and cytokine and nitric oxide production

[J]. *J Dairy Sci*, 2020, **103**(7): 5805-5815.

[50] Wu J. Tackle the free radicals damage in COVID-19 [J]. *Nitric Oxide*, 2020, **102**: 39-41.

[51] Ciaglia E, Malfitano AM, Laezza C*, et al.* Immuno-Modulatory and Anti-Inflammatory Effects of Dihydrogracilin A, a Terpene Derived from the Marine Sponge Dendrilla membranosa [J]. *Int J Mol Sci*, 2017, **18**(8).

[52] Talaat KR, Halsey NA, Cox AB*, et al.* Rapid changes in serum cytokines and chemokines in response to inactivated influenza vaccination [J]. *Influenza Other Respir Viruses*, 2018, **12**(2): 202-210.

[53] Barnes BJ, Adrover JM, Baxter-Stoltzfus A*, et al.* Targeting potential drivers of COVID-19: Neutrophil extracellular traps [J]. *J Exp Med*, 2020, **217**(6).

[54] Vardhana SA and Wolchok JD. The many faces of the anti-COVID immune response [J]. *J Exp Med*, 2020, **217**(6).

[55] Sumikoshi M, Hashimoto K, Kawasaki Y*, et al.* Human influenza virus infection and apoptosis induction in human vascular endothelial cells [J]. *Journal of medical virology*, 2008, **80**(6): 1072-1078.

[56] Teijaro John R, Walsh Kevin B, Cahalan S*, et al.* Endothelial Cells Are Central Orchestrators of Cytokine Amplification during Influenza Virus Infection [J]. *Cell*, 2011, **146**(6): 980-991.

[57] Kosai K, Seki M, Yanagihara K*, et al.* Elevated levels of high mobility group box chromosomal protein-1 (HMGB-1) in sera from patients with severe bacterial pneumonia coinfected with influenza virus [J]. *Scand J Infect Dis*, 2008, **40**(4): 338-342.

[58] Zheng J and Perlman S. Immune responses in influenza A virus and human coronavirus infections: an ongoing battle between the virus and host [J]. *Curr Opin Virol*, 2018, **28**: 43-52.

[59] Moisy D, Avilov SV, Jacob Y*, et al.* HMGB1 protein binds to influenza virus nucleoprotein and promotes viral replication [J]. *J Virol*, 2012, **86**(17): 9122-9133.

[60] Deng Y, Yang Z, Gao Y*, et al.* Toll-like receptor 4 mediates acute lung injury induced by high mobility group box-1 [J]. *PLoS One*, 2013, **8**(5): e64375.

[61] Fagone P, Shedlock DJ, Bao H*, et al.* Molecular adjuvant HMGB1 enhances anti-influenza immunity during DNA vaccination [J]. *Gene Ther*, 2011, **18**(11): 1070-1077.

[62] Tao X, Sun X, Yin L*, et al.* Dioscin ameliorates cerebral ischemia/reperfusion injury through the downregulation of TLR4 signaling via HMGB-1 inhibition [J]. *Free Radical Biology and Medicine*, 2015, **84**: 103-115.

[63] Sohn KM, Lee SG, Kim HJ*, et al.* COVID-19 Patients Upregulate Toll-like Receptor 4-mediated Inflammatory Signaling That Mimics Bacterial Sepsis [J]. *J Korean Med Sci*, 2020, **35**(38): e343.

[64] Wang QW, Su Y, Sheng JT*, et al.* Anti-influenza A virus activity of rhein through regulating oxidative stress, TLR4, Akt, MAPK, and NF-kappaB signal pathways [J]. *PLoS One*, 2018, **13**(1): e0191793.

[65] Dai JP, Wang QW, Su Y*, et al.* Emodin Inhibition of Influenza A Virus Replication and Influenza Viral Pneumonia via the Nrf2, TLR4, p38/JNK and NF-kappaB Pathways [J]. *Molecules*, 2017, **22**(10).

[66] Ren Z, Li J, Song X*, et al.* The regulation of inflammation and oxidative status against lung injury of residue polysaccharides by Lentinula edodes [J]. *Int J Biol Macromol*, 2018, **106**: 185-192.

[67] Diao JX, Ou JY, Dai H*, et al.* Antioxidant and Antiapoptotic Polyphenols from Green Tea Extract Ameliorate CCl4-Induced Acute Liver Injury in Mice [J]. *Chin J Integr Med*, 2020, **26**(10): 736-744.

[68] Koivisto AE, Olsen T, Paur I*, et al.* Effects of antioxidant-rich foods on altitude-induced oxidative stress and inflammation in elite endurance athletes: A randomized controlled trial [J]. *PLoS One*, 2019, **14**(6): e0217895.

[69] Chen J, Jin Y, Yang Y*, et al.* Epithelial Dysfunction in Lung Diseases: Effects of Amino Acids and Potential Mechanisms [J]. *Adv Exp Med Biol*, 2020, **1265**: 57-70.

[70] Tan L, Tu Y, Wang K*, et al.* Exploring protective effect of Glycine tabacina aqueous extract against nephrotic syndrome by network pharmacology and experimental verification [J]. *Chin Med*, 2020, **15**: 79.

[71] Khazdair MR and Boskabady MH. A double-blind, randomized, placebo-controlled clinical trial on the effect of carvacrol on serum cytokine levels and pulmonary function tests in sulfur mustard induced lung injury [J]. *Cytokine*, 2019, **113**: 311-318.

[72] Nakayama T, Kumagai T, Kashiwagi Y*, et al.* Cytokine production in whole-blood cultures following immunization with an influenza vaccine [J]. *Hum Vaccin Immunother*, 2018, **14**(12): 2990-2998.

[73] Rudd JM, Pulavendran S, Ashar HK*, et al.* Neutrophils Induce a Novel Chemokine Receptors Repertoire During Influenza Pneumonia [J]. *Front Cell Infect Microbiol*, 2019, **9**: 108.

[74] Wang W, Yang P, Zhong Y*, et al.* Monoclonal antibody against CXCL-10/IP-10 ameliorates influenza A (H1N1) virus induced acute lung injury [J]. *Cell Res*, 2013, **23**(4): 577-580.

[75] Chen S, Liu G, Chen J*, et al.* Ponatinib Protects Mice From Lethal Influenza Infection by Suppressing Cytokine Storm [J]. *Front Immunol*, 2019, **10**: 1393.

Table

Table.1 Constituents identified from INAE

Peak No.	Name Possible chemical	Categories	Formula	MS^1	MS^2
1	Adenine	Nucleosides	C5H5N5	136.13	119.00
2	2-Methyquinazlin-4(3H)-One	Alkaloids	C9H8N2O	161.14	140.84,133.20
3	Imidazolinones	Alkaloids	C8H7N3O	162.15	145.00
4	3-(2'-Hydroxyphenyl)-2-Methyl-4(3H)-Quinazolinone	Alkaloids	C15H12N2O2	253.16	134.09,120.06
5	Isaindigotone2	Alkaloids	C20H18N2O4	351.28	333.21,315.21
6	Adenosine	Nucleosides	C10H13N5O4	268.17	136.06
7	Annuionone D	Terpene	C13H20O3	225.18	156.28
8	6-Hydroxy-4-(5-Hydroxymethylfuran-2-yl)-Quinolin-2(1H)-One	Alkaloids	C16H19NO2	258.19	240.16
9	Valine	Amino acids	C15H11NO2	118.16	101.12,98.14
10	Hydroxylindirubin	Amino acids	C16H10N2O3	279.31	261.25,223.18
11	Isaindigodione	Alkaloids	C18H18N2O4	349.38	331.28
12	Mediroresinol	Alkaloids	C21H24O7	349.35	371.25
13	2-(3-Hydroxy)-4-Methoxy-2-Oxindolin-3-yl)-Acetamide	Alkaloids	C11H13N2O4	237.21	118.08
14	Ganine	Nucleosides	C5H5N5O	174.17	157.13
15	2-Hydroxy-1,4-Phthalate	Organic Acids	C8H6O5	183.16	163.06,139.12
16	Ethyl-3,4-Dihydro-4-Oxoquinazoline-2-Carboxylate	Alkaloids	C11H10N2O3	460.33	437.28,415.26

The phytochemical constituents in aqueous extract of indigo naturalis (INAE) were identified through UPLC-Q-TOF-MS and UPLC-LTQ-ESI-MS readouts including the retention time, MS/MS fragments, molecular form with referred to the databases SciFinder, PubChem, and Mass Bank.

Figures

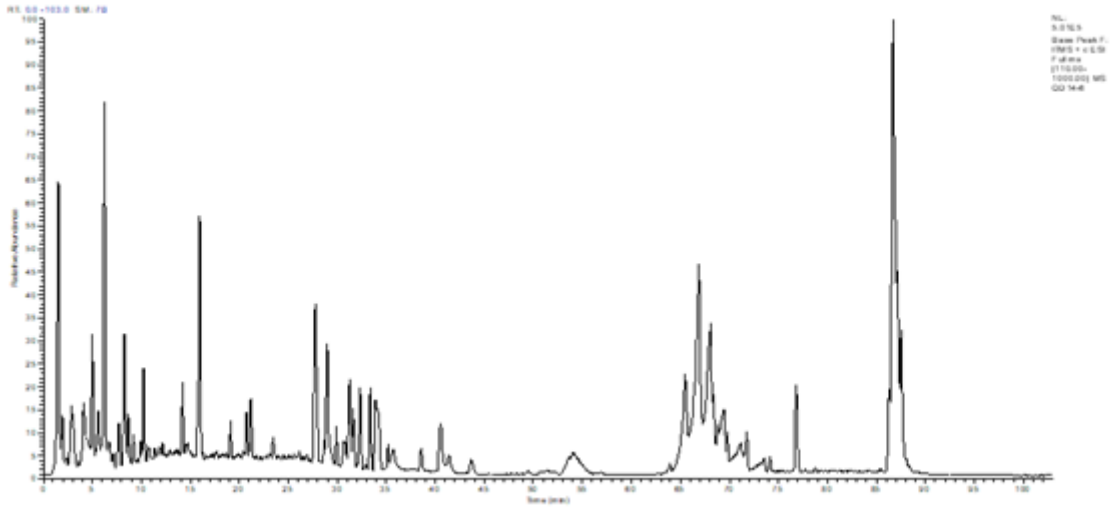

Figure 1

UPLC-ESI-LTQ-MS positive ion mode chromatogram of INAE The aqueous extract of indigo naturalis (INAE) was diluted in deionized water and filtered through a 0.22 μm filter before introduced to the UPLC-ESI-LTQ-MS analysis. A YMC-Triart C18 column was used with an injection volume of 5 μL for the constituent separation and analysis in positive ion mode.

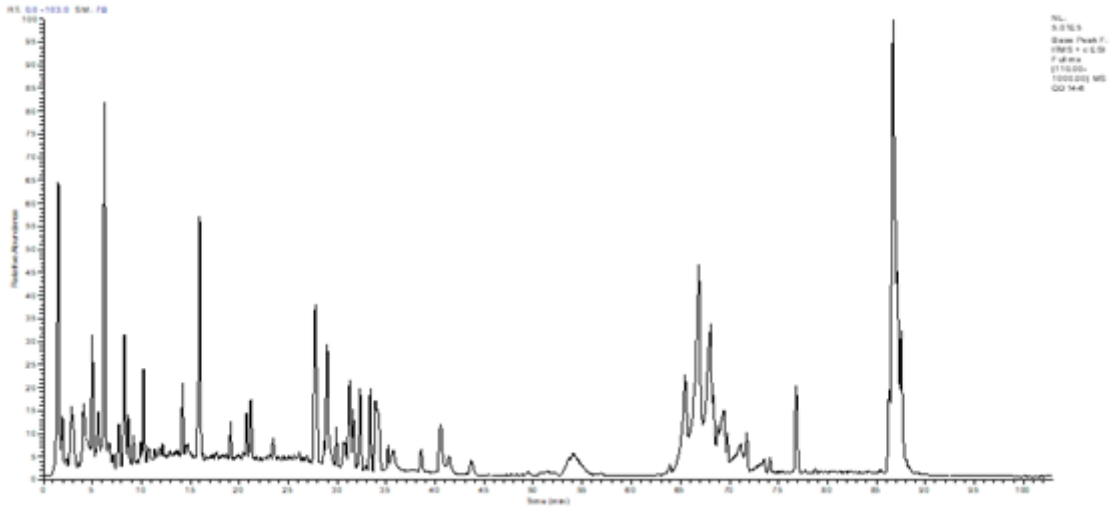

Figure 1

UPLC-ESI-LTQ-MS positive ion mode chromatogram of INAE The aqueous extract of indigo naturalis (INAE) was diluted in deionized water and filtered through a 0.22 μm filter before introduced to the UPLC-ESI-LTQ-MS analysis. A YMC-Triart C18 column was used with an injection volume of 5 μL for the constituent separation and analysis in positive ion mode.

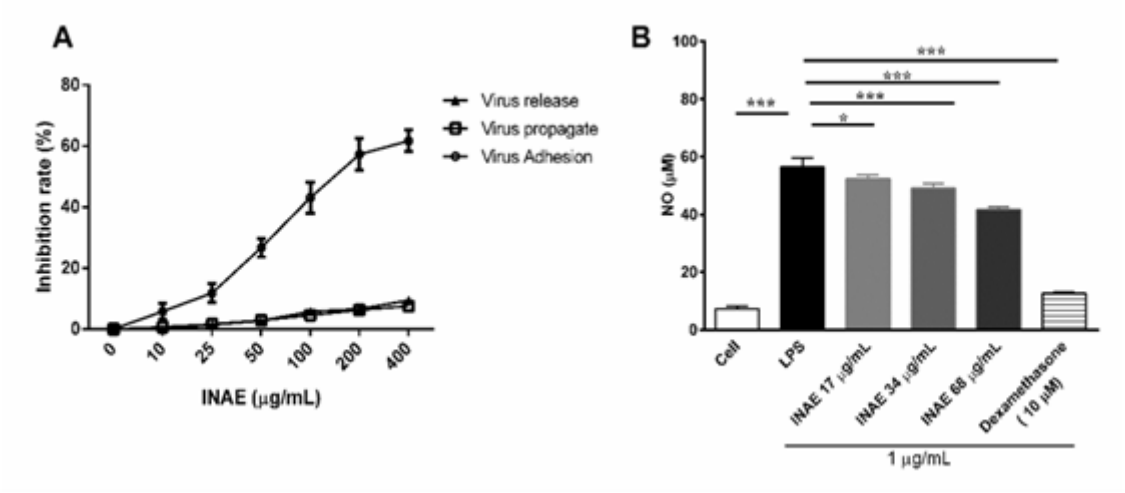

Figure 2

Anti-influenza and anti-inflammatory effect of INAE in vitro (A) Anti-influenza effect of INAE on MDCK cells. INAE was administrated 2 hours prior to, simultaneously, or 2 hours after influenza A virus infection to evaluate the antivirus capacity in phases of virus adhesion to cells, virus propagate in or release from the infected cells. (B) Effect of INAE on LPS induced nitric oxide (NO) production. LPS (1 μg/mL) was used as initiators in peritoneal macrophages and dexamethasone (10 μM) was used as positive control. Data were presented as mean ± S.D. (n = 4). * $P < 0.05$, *** $P < 0.001$ compared with LPS group, tested by ANOVA and Fisher's PLSD.

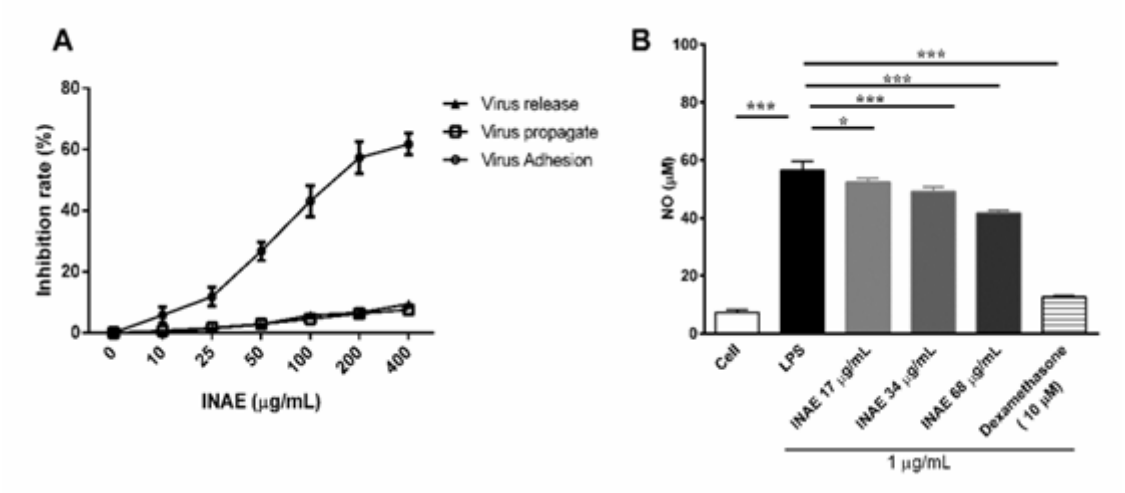

Figure 2

Anti-influenza and anti-inflammatory effect of INAE in vitro (A) Anti-influenza effect of INAE on MDCK cells. INAE was administrated 2 hours prior to, simultaneously, or 2 hours after influenza A virus infection to evaluate the antivirus capacity in phases of virus adhesion to cells, virus propagate in or release from the infected cells. (B) Effect of INAE on LPS induced nitric oxide (NO) production. LPS (1 μg/mL) was used as initiators in peritoneal macrophages and dexamethasone (10 μM) was used as positive control.

Data were presented as mean ± S.D. (n = 4). * P < 0.05, *** P < 0.001 compared with LPS group, tested by ANOVA and Fisher's PLSD.

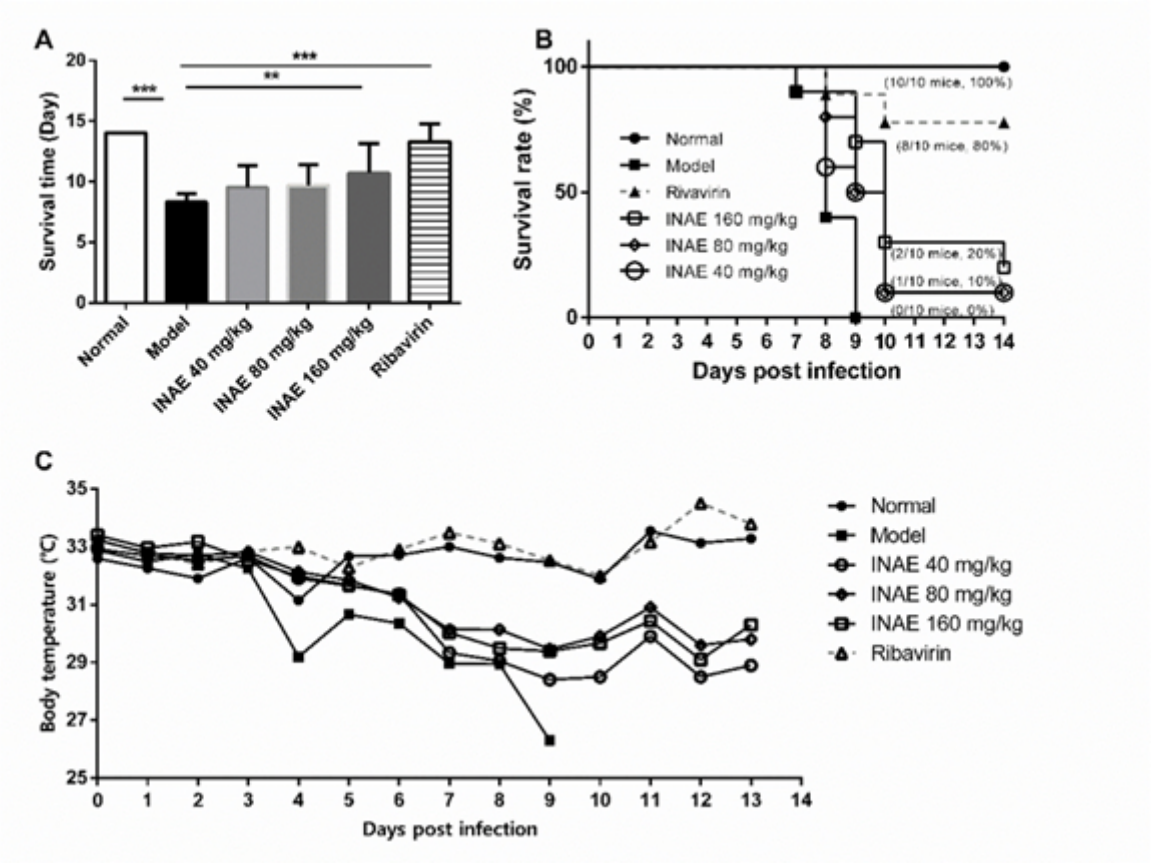

Figure 3

Effect of INAE on lifespan and survival rate of IAV-infected mice Mice were intranasally infected with 6 × LD50 of IAV and orally administered with INAE, ribavirin or 0.5% CMC-Na at indicated doses once daily for 7 days. Mice lifespan (A), survival rate (B), and mean body temperature during the study (C) were recorded. Data represent were expressed as mean ± S.D. (n = 10) ** P < 0.01, *** P < 0.001 compared with model group, tested by ANOVA and Fisher's PLSD.

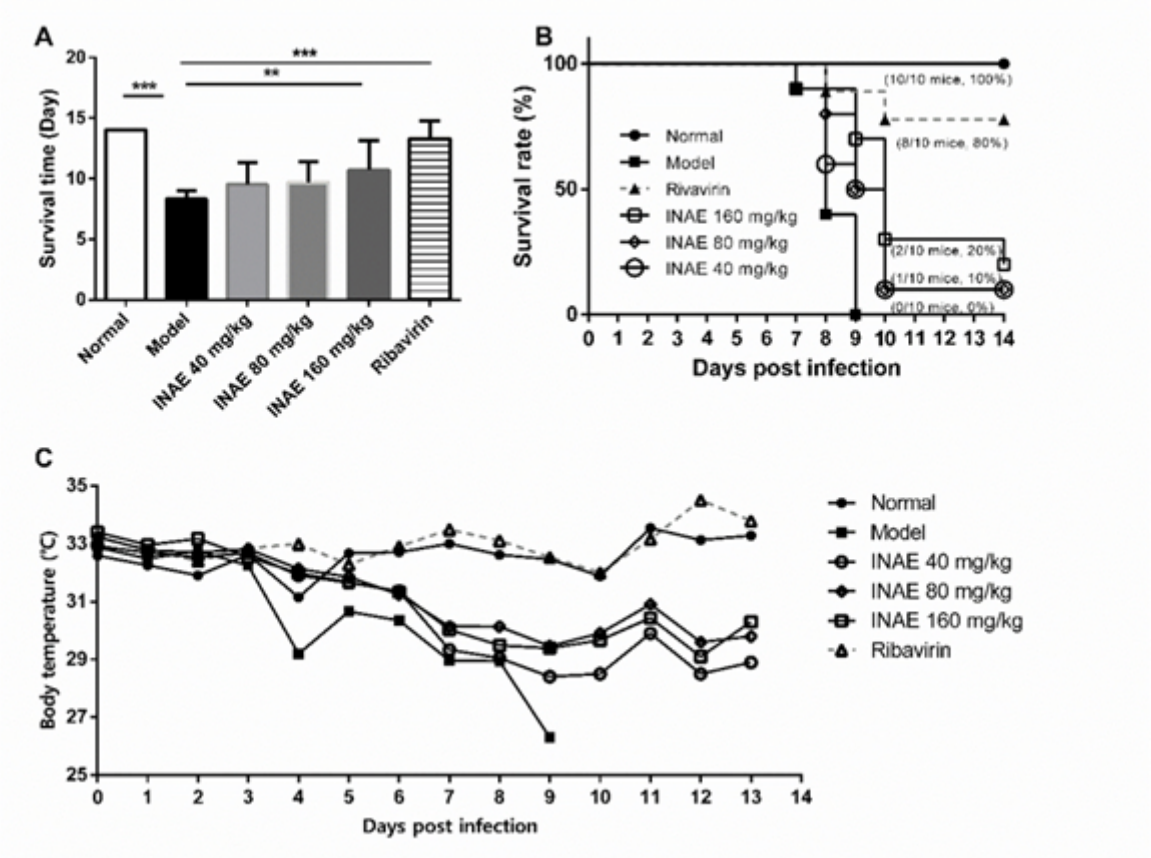

Figure 3

Effect of INAE on lifespan and survival rate of IAV-infected mice Mice were intranasally infected with 6 × LD50 of IAV and orally administered with INAE, ribavirin or 0.5% CMC-Na at indicated doses once daily for 7 days. Mice lifespan (A), survival rate (B), and mean body temperature during the study (C) were recorded. Data represent were expressed as mean ± S.D. (n = 10) ** $P < 0.01$, *** $P < 0.001$ compared with model group, tested by ANOVA and Fisher's PLSD.

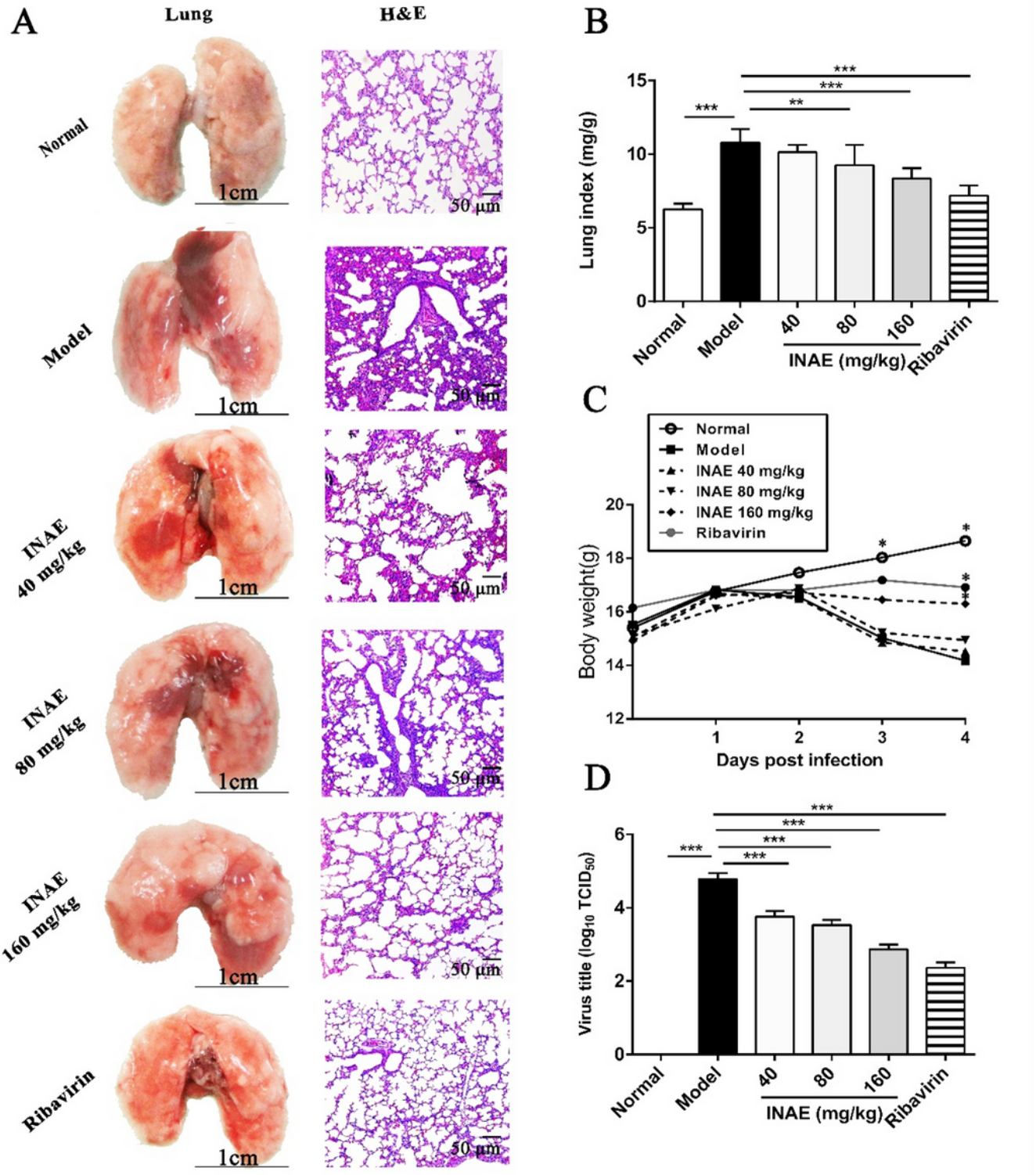

Figure 4

. Effect of INAE on lung injury, lung index, body weight and virus titer of IAV-infected mice Mice were infected with 3 × LD50 of IAV and orally administered with INAE, ribavirin or 0.5% CMC-Na at indicated doses once daily for 4 days. Lung index, mice body weight, and virus titer were calculated and detected. Lung photos and hematoxylin-eosin stain (H&E) with vision of 200 × (A). Lung index = Lung weight / body weight × 100% (B). Mice body weight growth curve (C). Virus titer in lung homogenate of mice (D).

Data were presented as mean ± S.D. (n = 6). ** P < 0.01, *** P < 0.001 compared with model group, tested by ANOVA and Fisher's PLSD.

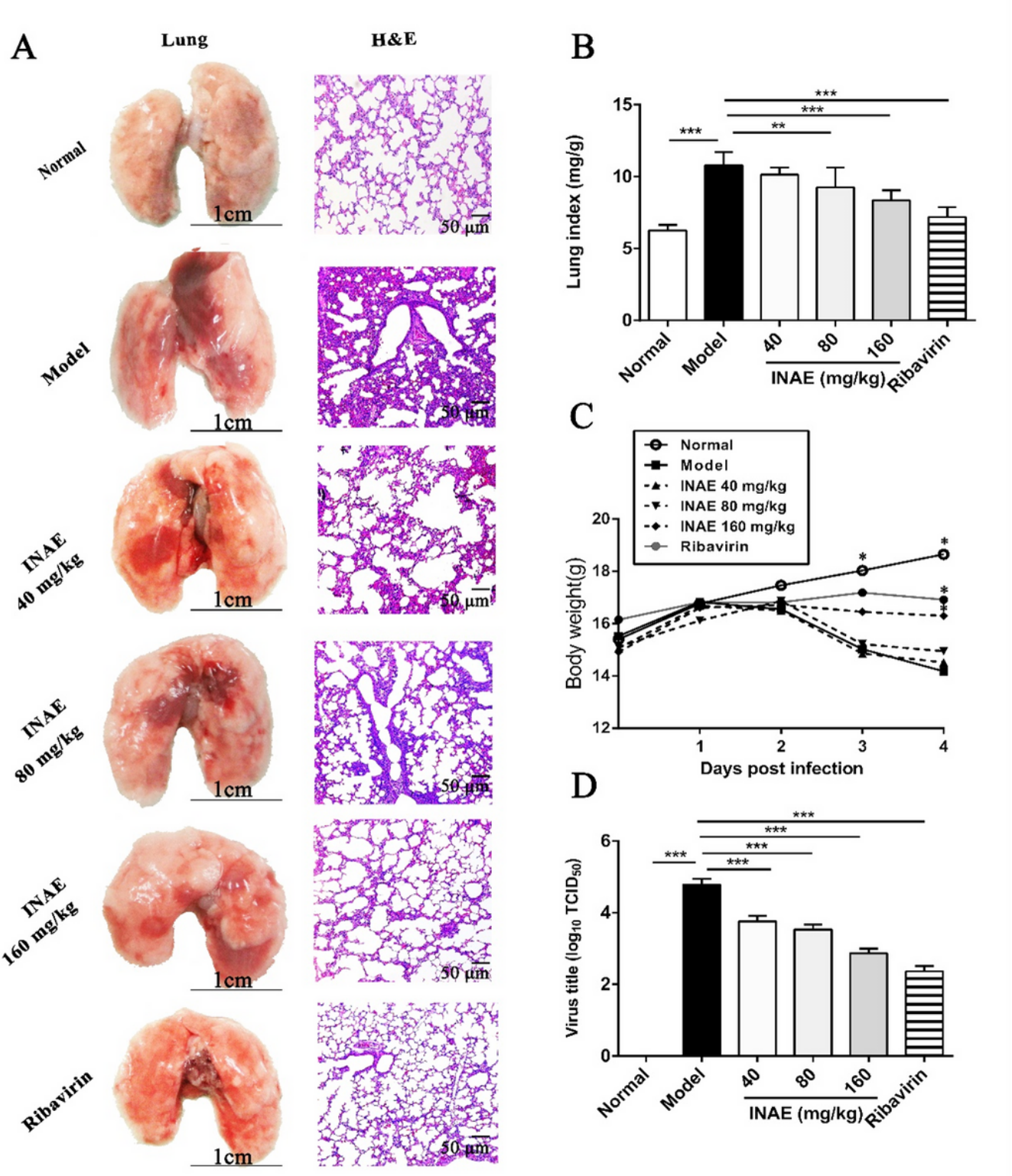

Figure 4

. Effect of INAE on lung injury, lung index, body weight and virus titer of IAV-infected mice Mice were infected with 3 × LD50 of IAV and orally administered with INAE, ribavirin or 0.5% CMC-Na at indicated doses once daily for 4 days. Lung index, mice body weight, and virus titer were calculated and detected.

Lung photos and hematoxylin-eosin stain (H&E) with vision of 200 × (A). Lung index = Lung weight / body weight × 100% (B). Mice body weight growth curve (C). Virus titer in lung homogenate of mice (D). Data were presented as mean ± S.D. (n = 6). ** P < 0.01, *** P < 0.001 compared with model group, tested by ANOVA and Fisher's PLSD.

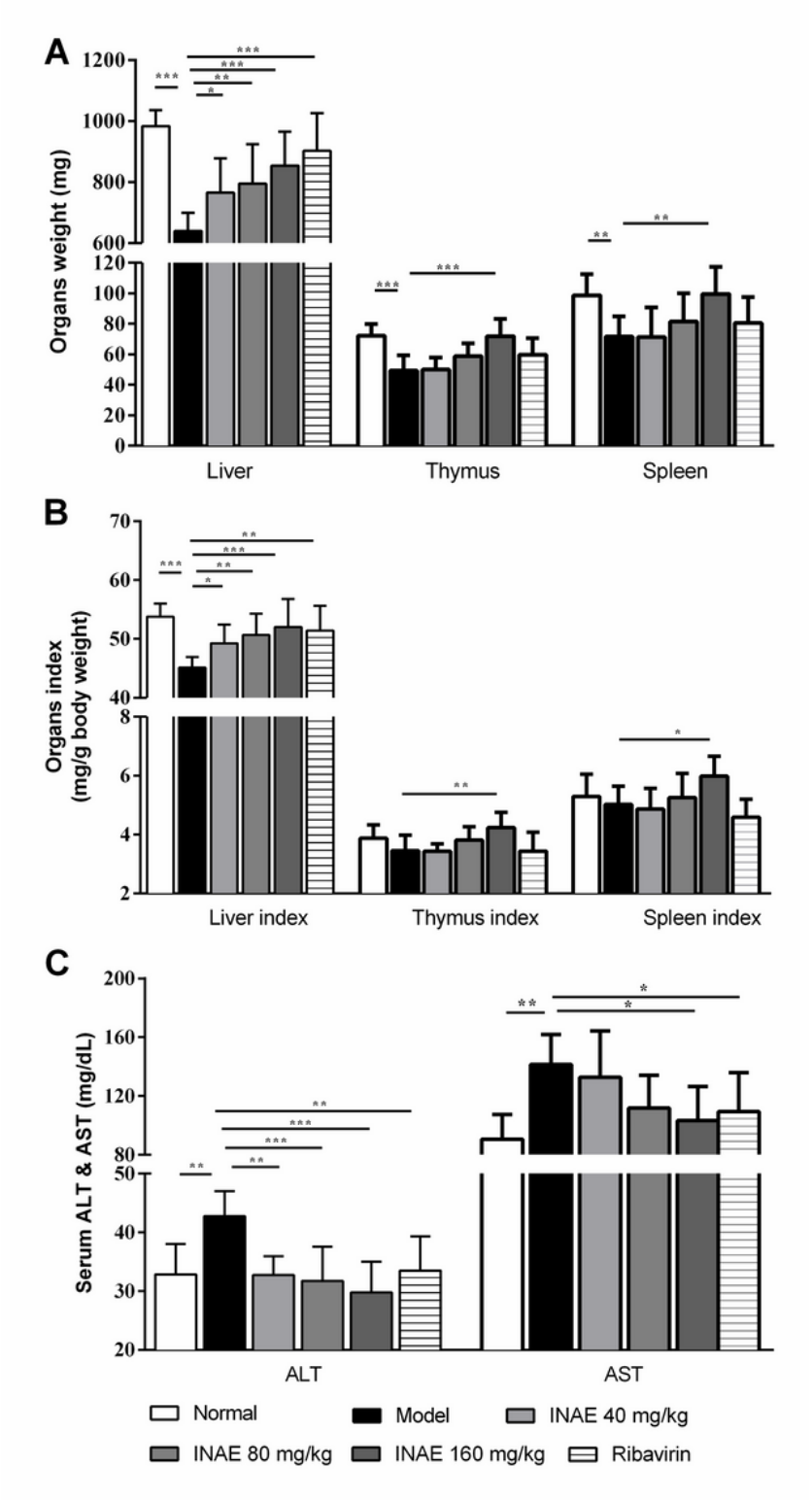

Figure 5

Effect of INAE on liver, thymus and spleen Mice were infected with 3 × LD50 of IAV and orally administered with INAE, ribavirin or 0.5% CMC-Na at indicated doses once daily for 4 days. Weights of liver, thymus and spleen were measured and calculated (A ~ B). Serum ALT and AST levels were evaluated (C). Organ index = Organ weight / body weight × 100%. Data were presented as mean ± S.D. (n = 6). * P < 0.05, ** P < 0.01, *** P < 0.001 compared with model group, tested by ANOVA and Fisher's PLSD.

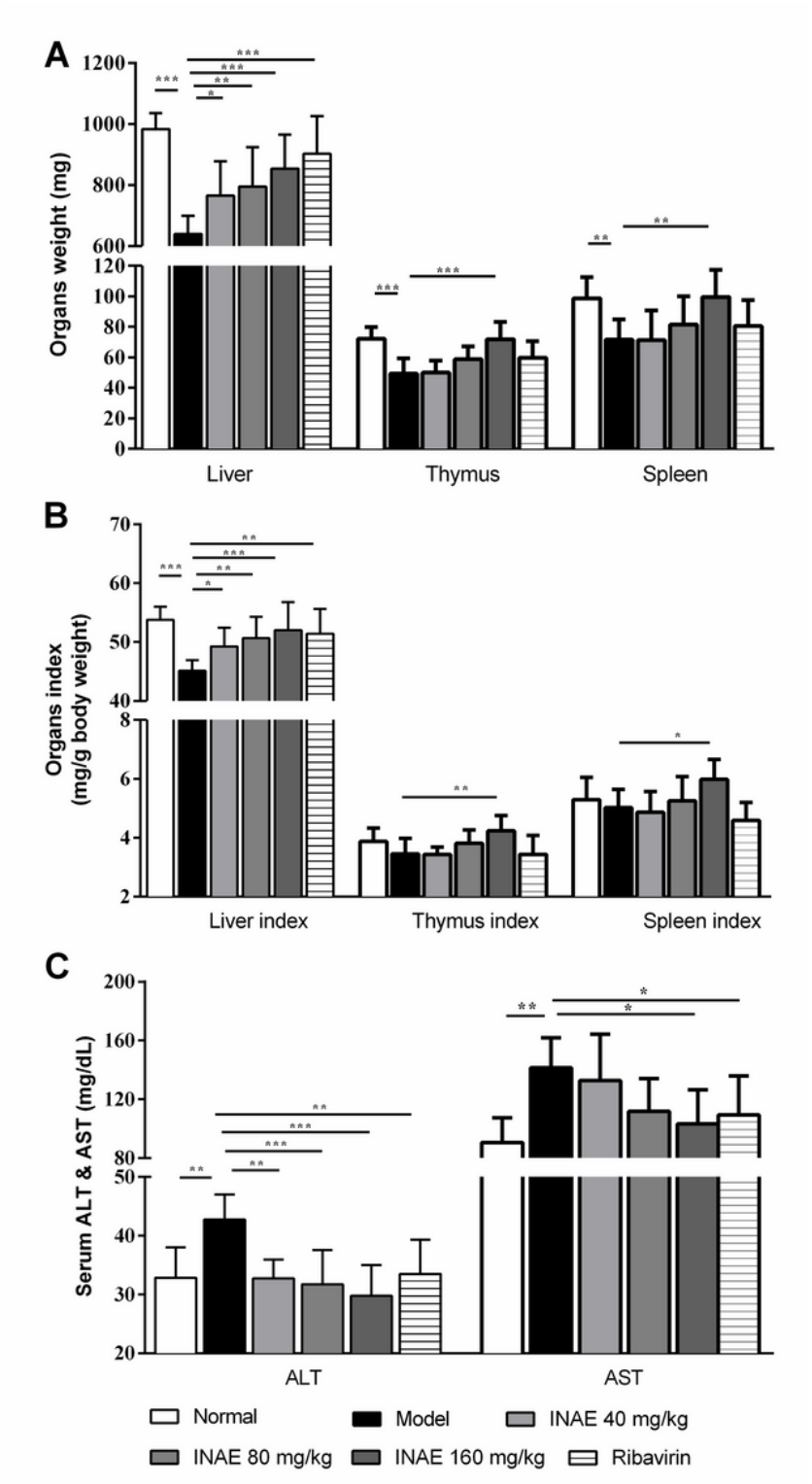

Figure 5

Effect of INAE on liver, thymus and spleen Mice were infected with 3 × LD50 of IAV and orally administered with INAE, ribavirin or 0.5% CMC-Na at indicated doses once daily for 4 days. Weights of liver, thymus and spleen were measured and calculated (A ~ B). Serum ALT and AST levels were evaluated (C). Organ index = Organ weight / body weight × 100%. Data were presented as mean ± S.D. (n = 6). * P < 0.05, ** P < 0.01, *** P < 0.001 compared with model group, tested by ANOVA and Fisher's PLSD.

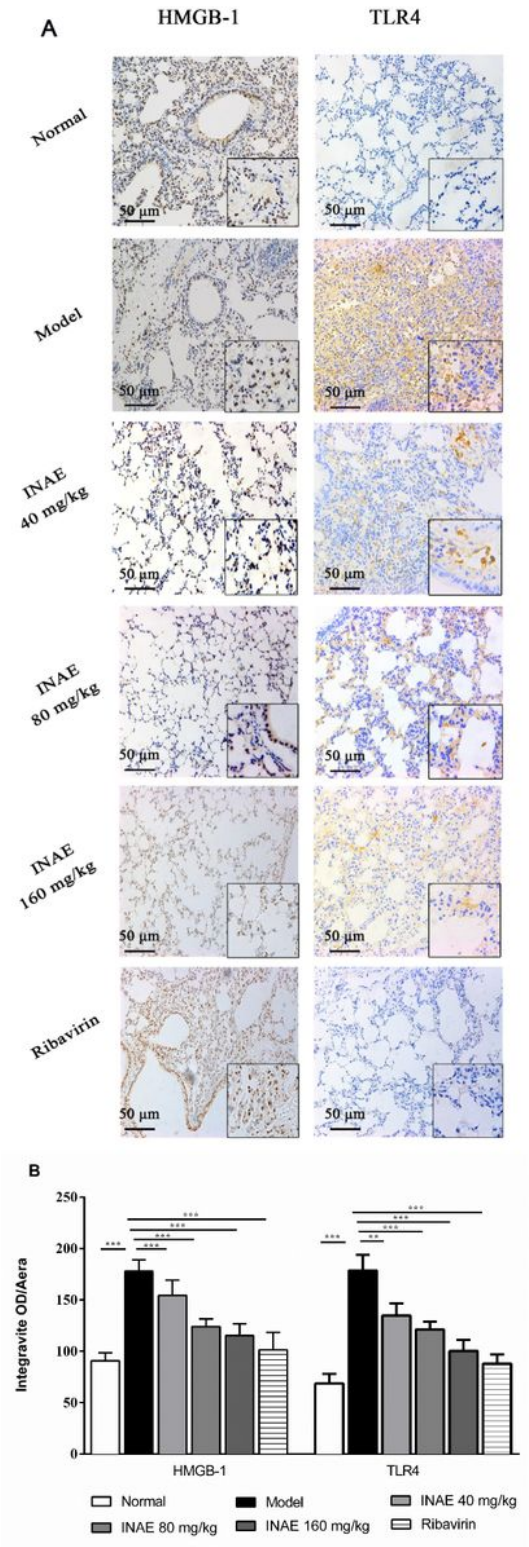

Figure 6

HMGB-1 and TLR4 expression in lung of IAV-infected mice Lung tissues of IAV infected mice were harvested, fixed in formalin, and embedded in paraffin and processed for slices preparation. (A)The slides were incubated with relative antibodies against HMGB-1 and TLR4, stained with chromogenic substrate solution and counterstained with hematoxylin. The immuno-histochemical (200 ×) of expression of HMGB-1 and TLR4 in lung of IAV infected mice were visualized under a microscope. (B) The expression of HMGB-1 and TLR4 were assessed by semi-quantitative analysis using ImageJ software. The levels of HMGB-1 or TLR4 were expressed as average optical value (AOD) (n = 4). AOD = Integrative density of optical value / Aera.

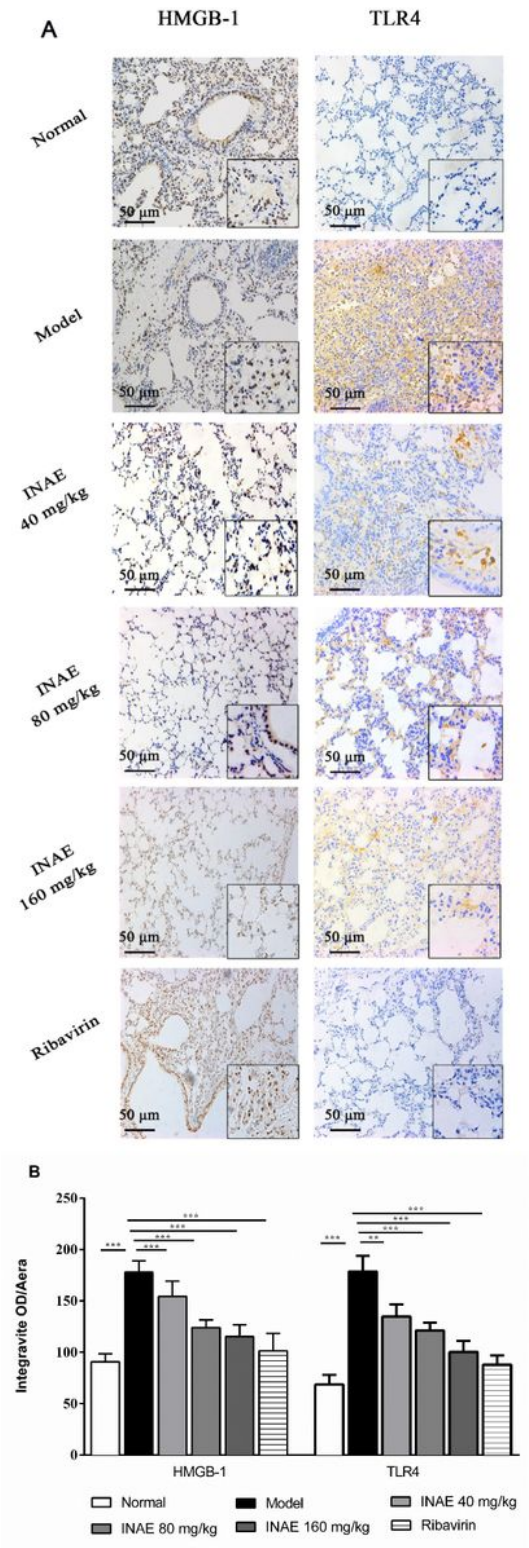

Figure 6

HMGB-1 and TLR4 expression in lung of IAV-infected mice Lung tissues of IAV infected mice were harvested, fixed in formalin, and embedded in paraffin and processed for slices preparation. (A)The slides were incubated with relative antibodies against HMGB-1 and TLR4, stained with chromogenic substrate solution and counterstained with hematoxylin. The immuno-histochemical (200 ×) of expression of HMGB-1 and TLR4 in lung of IAV infected mice were visualized under a microscope. (B) The expression

of HMGB-1 and TLR4 were assessed by semi-quantitative analysis using ImageJ software. The levels of HMGB-1 or TLR4 were expressed as average optical value (AOD) (n = 4). AOD = Integrative density of optical value / Aera.

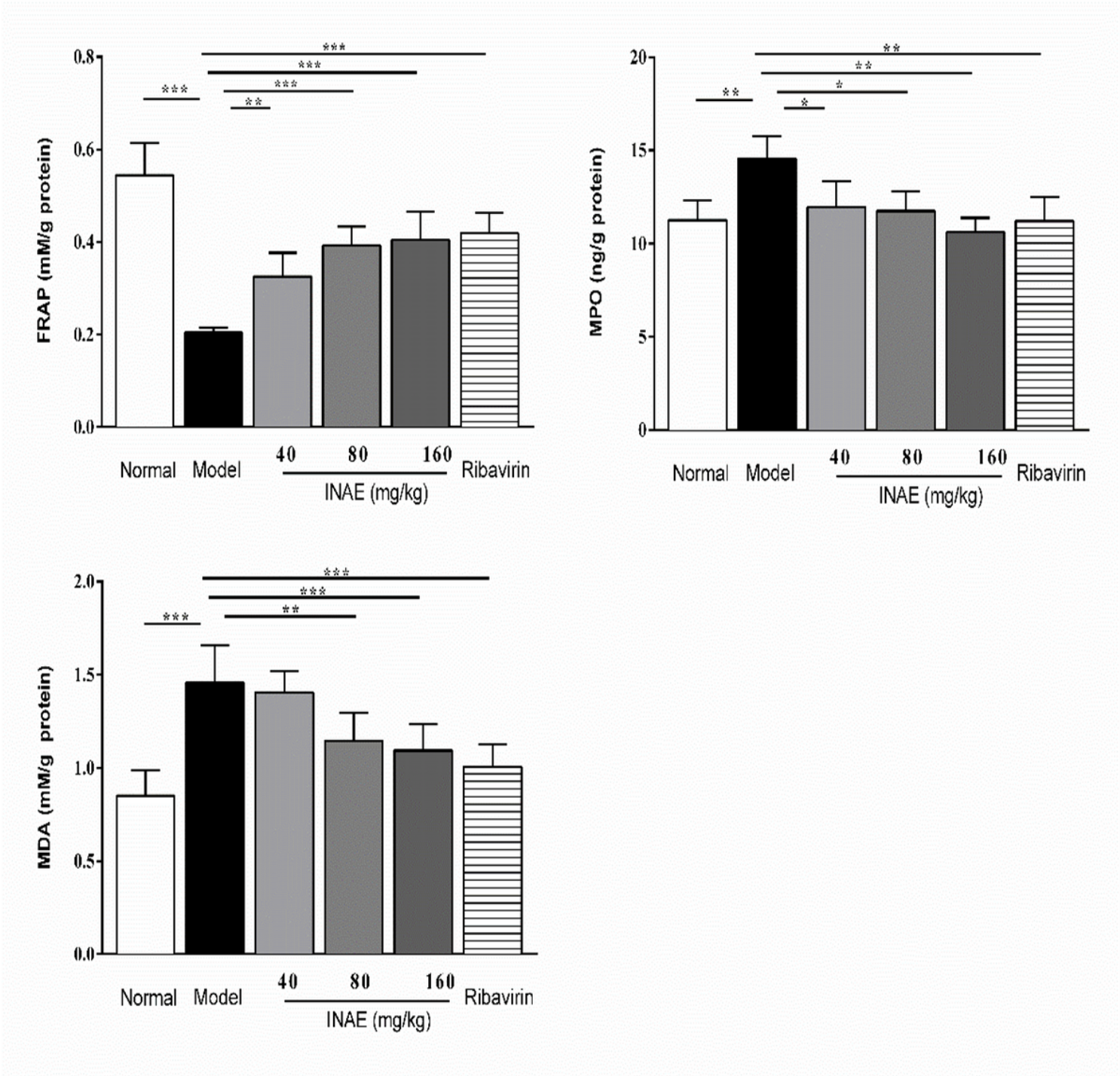

Figure 7

Anti-oxidant effect of INAE in lung of IAV-infected mice (A) Ferric ion reducing antioxidant power (FRAP), (B) Myeloperoxidase (MPO) and (C) Malonaldehyde (MDA) in lung homogenate of IAV infected mice were analyzed to evaluate the effect of INAE on oxidant stress reaction. Data were expressed as mean ± S.D. (n

= 6). * P < 0.05, ** P < 0.01, *** P < 0.001 compared with model group, tested by ANOVA and Fisher's PLSD.

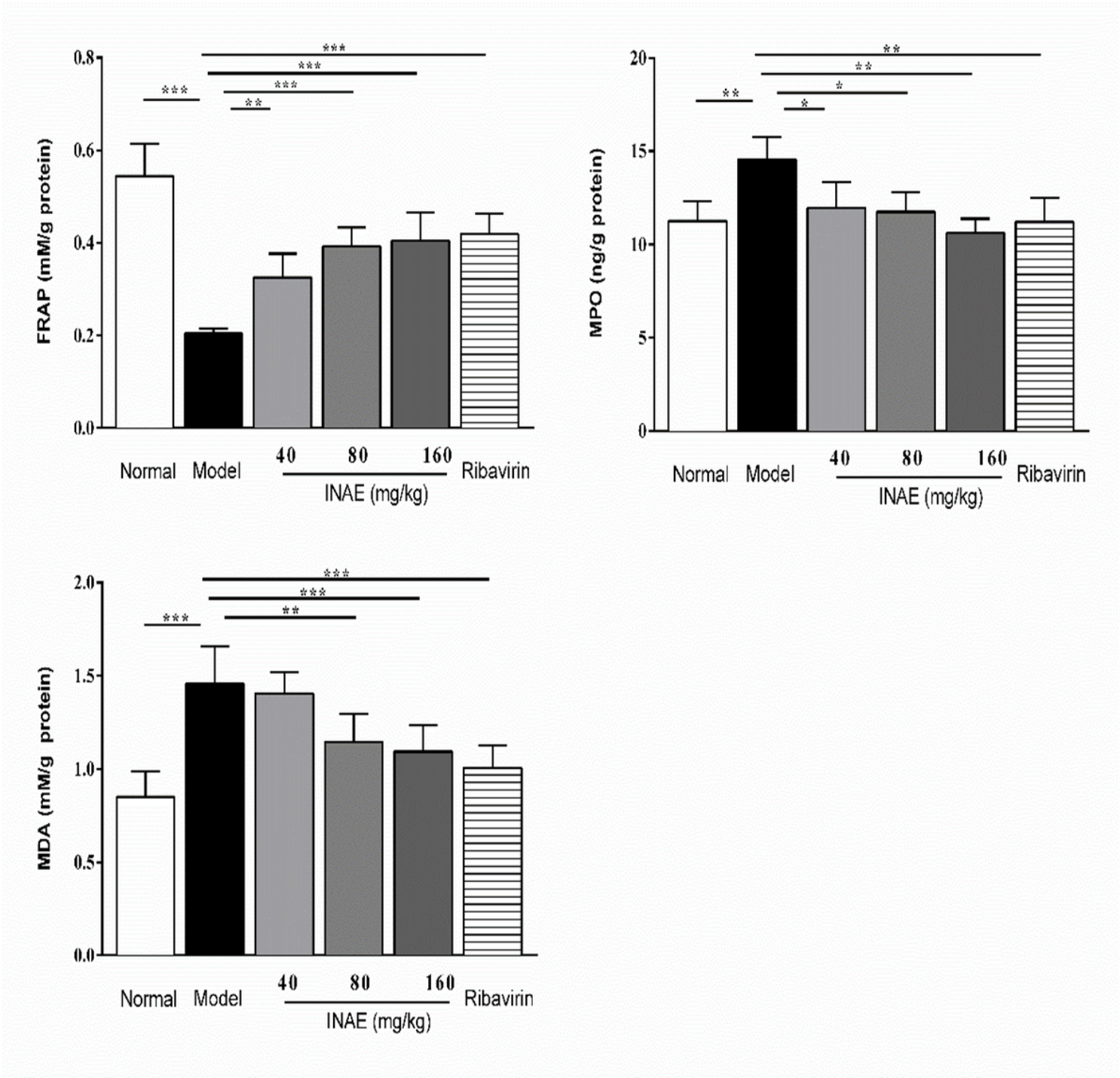

Figure 7

Anti-oxidant effect of INAE in lung of IAV-infected mice (A) Ferric ion reducing antioxidant power (FRAP), (B) Myeloperoxidase (MPO) and (C) Malonaldehyde (MDA) in lung homogenate of IAV infected mice were analyzed to evaluate the effect of INAE on oxidant stress reaction. Data were expressed as mean ± S.D. (n = 6). * P < 0.05, ** P < 0.01, *** P < 0.001 compared with model group, tested by ANOVA and Fisher's PLSD.

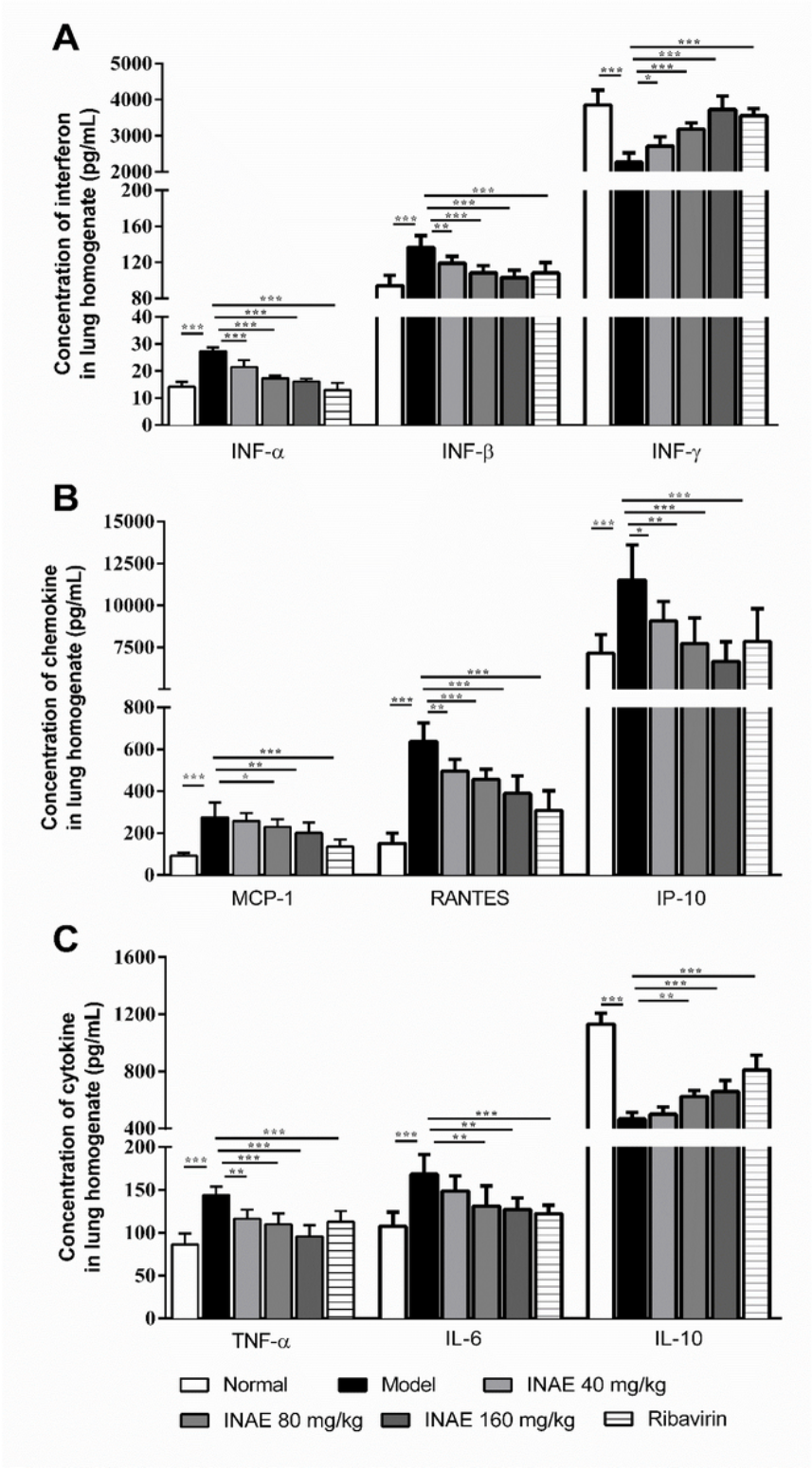

Figure 8

Interferon, chemokine and cytokine levels in lung of IAV-infected mice Effect of INAE on inflammation response in IAV infected mice were detected at day 4 after IAV infection. Interferon IFN-α, IFN-β, and INF-γ (A), MCP-1, RANTES and IP-10 (B), and TNF-α, IL-6, and IL-10 (C) levels were evaluated. Data were expressed as mean ± S.D. (n = 6). * $P < 0.05$, ** $P < 0.01$, *** $P < 0.001$ compared with model group, tested by ANOVA and Fisher's PLSD.

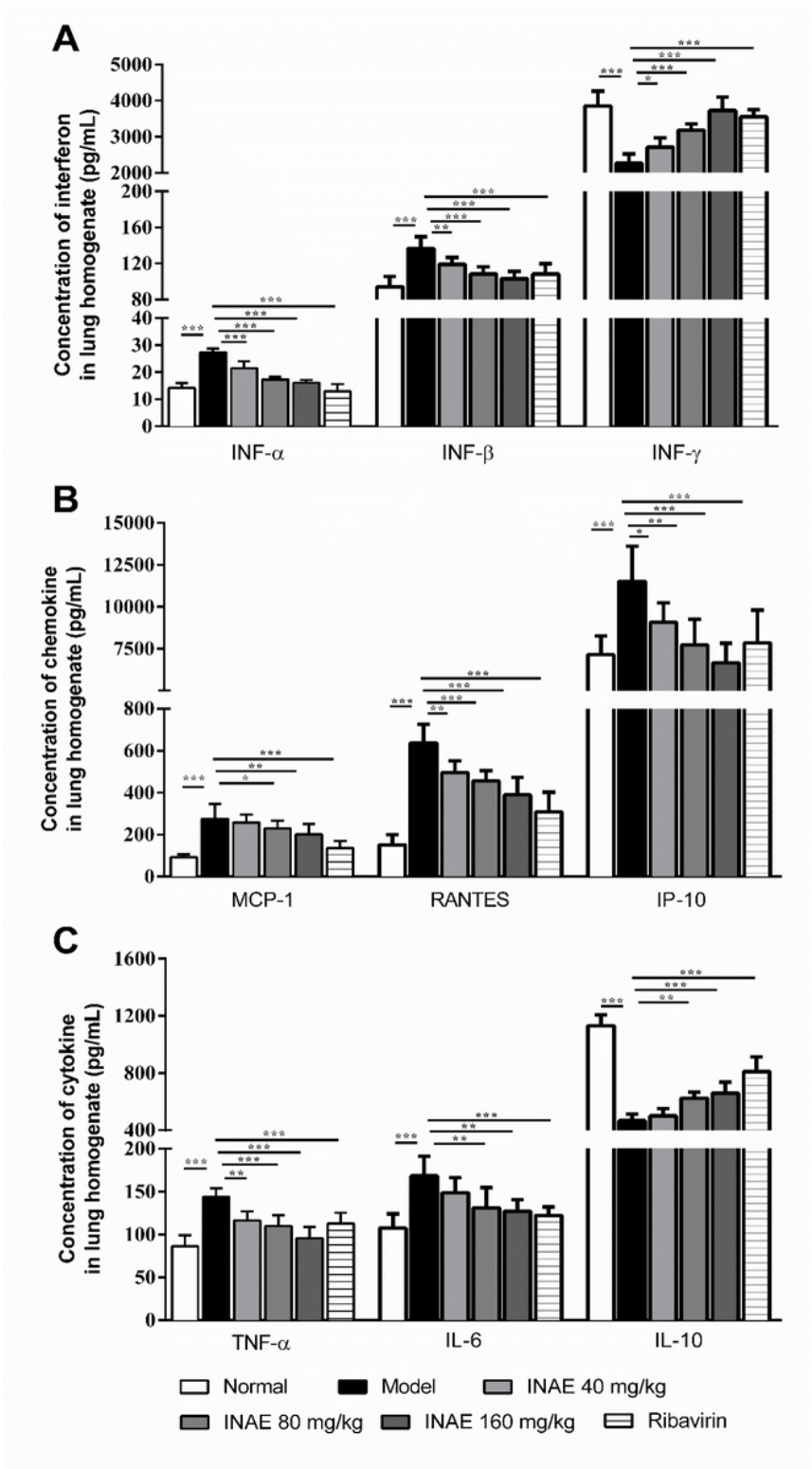

Figure 8

Interferon, chemokine and cytokine levels in lung of IAV-infected mice Effect of INAE on inflammation response in IAV infected mice were detected at day 4 after IAV infection. Interferon IFN-α, IFN-β, and INF-γ (A), MCP-1, RANTES and IP-10 (B), and TNF-α, IL-6, and IL-10 (C) levels were evaluated. Data were expressed as mean ± S.D. (n = 6). * $P < 0.05$, ** $P < 0.01$, *** $P < 0.001$ compared with model group, tested by ANOVA and Fisher's PLSD.

Supplementary Files

This is a list of supplementary files associated with this preprint. Click to download.

- Fig9.png
- Fig9.png
- Supplymentmaterialforreview.doc
- Supplymentmaterialforreview.doc